A&A manuscript no.
(will be inserted by hand later)

Your thesaurus codes are:
03(02.01.2; 02.13.1; 02.16.1; 11.01.2; 11.10.1; 11.14.1)

ASTRONOMY AND ASTROPHYSICS
29.6.1995

The jet-disk symbiosis

I. Radio to X-ray emission models for quasars

Heino Falcke and Peter L. Biermann

Max-Planck Institut für Radioastronomie, Auf dem Hügel 69, D-53121 Bonn, Germany

Astronomy & Astrophysics 293, 665

Abstract. Starting from the assumption that radio jets and accretion disks are symbiotic features present in radio loud and radio quiet quasars we scale the bulk power of radio jets with the accretion power by adding mass- and energy conservation of the whole jet-disk system to the standard Blandford & Königl theory for compact radio cores. The jet is described as a conically expanding plasma with maximal sound speed $c/\sqrt{3}$ enclosing relativistic particles and a magnetic field. Relativistic speeds of $\gamma_{\rm j}\beta_{\rm j} \gtrsim 5$ make an additional confinement unnecessary and the shape is solely given by the Mach cone. The model depends on only few parameters and can be constrained by observations. Thus we are able to show that radio and X-ray fluxes (SSC emission) of cores and lobes and typical dimensions of radio loud quasars are consistent with a jet being produced in the central engine. We present a synthetic broadband spectrum from radio to X-ray for a jet-disk system. The only way to explain the high efficiency of radio loud objects is to postulate that these objects consist of 'maximal jets' with 'total equipartition' where the magnetic energy flow of the jet is comparable to the kinetic jet power and the total jet power is a large fraction of the disk power. As the number of electrons is limited by the accretion flow, such a situation is only possible when the minimum Lorentz factor of the electron distribution is $\gamma_{\rm e,min} \gtrsim 100$ ($E \gtrsim 50$MeV) or/and a large number of pairs are present. Such an electron/positron population would be a necessary consequence of hadronic interactions and may lead to some interesting effects in the low frequency self-absorbed spectrum. Emission from radio weak quasars can be explained with an initially identical jet. The difference between radio loud and radio weak could be due to a different efficiency in accelerating relativistic electrons on the sub-parsec scale only. Finally we demonstrate that in order to appease the ravenous hunger of radio loud jets its production must be somehow linked to the dissipation process in the inner part of the disk.

Send offprint requests to: HFALCKE@mpifr-bonn.mpg.de

Key words: accretion disks – plasmas – magnetic fields – galaxies: active – galaxies: jets – galaxies: nuclei

1. Introduction

Some of the most spectacular objects in astrophysics are the giant radio lobes and jets found in many active galaxies. Today it is fairly well established that these structures are due to a collimated outflow from the nuclear region. High resolution studies show jet-like structures on all scales with a common alignment (Bridle & Perley 1984), suggesting that indeed the jet is accelerated on small scales and proceeds through the galaxy until it is stopped far from the nucleus. In the most active galaxies – the quasars – the radio spectrum of the jet may dominate the whole radio emission of the galaxy. However, only $\sim 10\%$ of the quasars show radio jets on large (>10 kpc) scales, even though nuclear radio emission is found in many more objects (Kellermann et al. 1989).

Another feature of active galactic nuclei (AGN) is an enormous energy output in other wavelengths as well, coming from an extremely compact core. An average spectrum consists of two important components, an infrared (IR) bump and an ultraviolet (UV) bump (Sanders et al. 1989). The latter can be fitted by emission from a standard accretion disk (Shakura & Sunyaev 1973, Novikov & Thorne 1973) around a supermassive black hole with mass $M_\bullet > 10^7 M_\odot$ accreting $0.1 - 10 M_\odot$/yr (Sun & Malkan 1989). In recent years it became clear that beyond these parts also in the X-ray and γ-ray region important contributions to the overall AGN luminosity can be found (e.g. Hartman et al. 1992). The presence of reflected components in the disk spectra lead to a modification of the simple accretion disk scenario, where the disk is additionally heated by an external source, probably powered by the nuclear jet (Niemeyer & Biermann 1993) or a disk corona (Haardt et al. 1991).

An obvious conclusion of the presence of accretion disk and radio jet is the idea that both are intimately linked: the jet is produced in the inner parts of the disk and flows along its rotation axis outwards. And indeed, Rawlings & Saunders (1991) found a remarkable correlation between a disk luminosity indicator and the power of the large scale jet structures in FRII galaxies.

But despite many attempts to model this, the origin and acceleration mechanism of jets is still uncertain. This is mainly due to the fact that the acceleration region is hidden deep inside the quasar, so that the boundary conditions for any theory are arbitrary over a wide range. Our approach now is to construct a more descriptive model based on the standard theory for the emission from compact radio cores by Blandford & Königl (1979, see also Marscher 1992 for a recent review) to which we simply add mass and energy conservation of the jet-disk system. This model can be constrained by observations and provides us with information about possible physical states of the jet plasma.

Our work is split in several parts. In this paper (Paper I) we discuss the underlying model of an electron(/positron)/proton plasma jet linked to an accretion disk within a standard set of parameters. Section 2 describes the properties of the jet plasma and defines model parameters. In Sec. 3 we calculate the observable consequences in radio wavelengths of such models which are discussed in Sec. 6. Section 4 discusses the expected X-ray signature from SSC emission and Sec. 5 contains some remarks concerning the standard accretion disk theory and possible mechanisms for the jet production. In a second paper (Falcke et al. 1994, Paper II) we test the predictions of our model with the optically selected PG sample of bright quasars and in a third paper (Falcke & Biermann 1994; also Falcke 1994) we will test our hypothesis for galactic sources.

2. Jet-disk symbiosis

Falcke et al. (1993a, b) and Falcke & Biermann (1993) developed a jet-disk model for the center of the Milky Way to explain the radio to near-infrared-spectrum of the supermassive black hole candidate Sgr A*. They predict the presence of a weak jet on the milli-arcsecond (mas) to sub-mas scale in Sgr A* as the consequence of a low accretion rate onto a rotating black hole. This is strengthened by recent VLBI observations of this source at 7mm (Krichbaum et al. 1993), where for the first time this source was partially resolved and shows an elongated structure.

We now want to extend this analysis to other objects as well and generalize our hypothesis to make it even stronger. Here we start with the basic ansatz that *jet and disk are symbiotic features.* This makes the link hypothesis bi-directional: not only is a disk required to produce a jet, also does the disk need a jet to fulfill its inner boundary conditions. One has to admit, there is no strong physical justification for this assumption, besides the perception that indeed standard accretion disk theory breaks down in the very inner region close to the black hole, but we rather start with the most comprehensive approach, calculate the expected observational signatures and then let observation decide when, where and how far one has to step back to get more specific theories. Our 'symbiosis' ansatz thereby implies that also the radio weak quasars produce radio jets in which energetic particles are accelerated as was proposed earlier to explain IR observations (Chini et al. 1989a, Niemeyer & Biermann 1993).

2.1. The link

Within such a jet-disk model, we express the basic properties of the radio jet in units of the disk accretion rate $\dot{M}_{\rm disk}$ and the mass $M_\bullet$ of the black hole. We use the same notation as in Falcke et al. (1993b). The maximum accretion power $Q_{\rm accr}$ is given by the rest energy at infinity of the matter $\dot{M}_{\rm disk}c^2$. The total radiated disk luminosity $L_{\rm disk}$ is an appreciable fraction $q_{\rm l}$ of this accretion power and for a black hole will be in the range $q_{\rm l} \sim 5\% - 30\%$ (Thorne 1974). Likewise, the total jet power $Q_{\rm jet}$ – including the rest energy of the expelled matter – should be a fraction $q_{\rm j} < 1$ of the accretion power and also the mass loss rate due to the jet $\dot{M}_{\rm jet}$ is a fraction $q_{\rm m} < 1$ of the mass accretion rate in the disk. Thus we define

$$q_{\rm j} = \frac{Q_{\rm jet}}{\dot{M}_{\rm disk}c^2}, \qquad q_{\rm l} = \frac{L_{\rm disk}}{\dot{M}_{\rm disk}c^2}, \qquad q_{\rm m} = \frac{\dot{M}_{\rm jet}}{\dot{M}_{\rm disk}}. \tag{1}$$

The $q_{\rm d,j,m}$ are dimensionless parameters, while $\dot{M}_{\rm disk}c^2$ defines the absolute energy scale of the system; c denotes the speed of light. We neglect all other energy consuming processes so that the remaining energy $(1 - q_{\rm j} - q_{\rm l})\dot{M}_{\rm disk}c^2$ is swallowed by the black hole. To scale the equations for AGN, we will refer to the following standard masses and accretion rates:

$$m_8 = \frac{M_\bullet}{10^8 M_\odot} \tag{2}$$

$$\dot{m}_{\rm disk} = \frac{\dot{M}_{\rm disk}}{1\, M_\odot/{\rm yr}}. \tag{3}$$

The total luminosity of a disk around a maximally rotating black hole with Kerr parameter $a = 0.9981$ is $L_{\rm disk} = 1.7 \cdot 10^{46} \dot{m}_{\rm disk}$ erg/sec and the (spherical) Eddington luminosity of the black hole is $L_{\rm edd} = 1.26 \cdot 10^{46}\, m_8$ erg/sec.

In our model the base of the jetflow is close to or at the boundary layer between accretion disk and black hole. The characteristic length scale of the jet-disk system is the characteristic scale of the Black Hole: the gravitational radius $R_{\rm g} = GM_\bullet/c^2 = 1.48 \cdot 10^{13}\, m_8$cm. In the following we will use small letters to represent dimensionless variables, e.g. we will write the radial coordinate R and the vertical (along the jet) coordinate Z as

$$r_{\rm jet} = R_{\rm jet}/R_{\rm g}, \quad z_{\rm jet} = Z_{\rm jet}/R_{\rm g} \tag{4}$$

The jet will split in four basic parts. First, the flow will be accelerated in a nozzle close to the disk, then it will expand adiabatically, enclosing the magnetic field and showing up as the flat spectrum core, after that we expect an intermediate phase, where ordered magnetic fields and shocks dominate the structure which can be seen as a jet like in M87 and finally the flow will either become subsonic and terminate in the interstellar medium (ISM) or further out in the intergalactic medium (IGM) producing lobes and hotspots. Accordingly we will refer to the four regions as jet nozzle, inner jet cone, outer jet cone and lobe.

2.2. Initial conditions of the jet plasma

In this subsection we discuss the initial conditions of the supersonic jetflow in or right after the nozzle. The prerequisite of this model is that the jet is described by a plasma accelerated close to the disk, containing a magnetic field and a population of relativistic electrons and protons with a power-law distribution. The acceleration zone is assumed to be very small as is the case in most hydrodynamical and hydromagnetic winds, so that the jet velocity $\beta_{\rm j}c$ is treated as being constant. The magnetic field is produced in or close to the disk. Relativistic particles are assumed to be produced in the jet somewhere between the disk and the first visible emission ($\lesssim 10^{17}$ cm) by a process related to the magnetic field; diffusive shock acceleration is just one example of such a process. Hereafter, all hydrodynamical quantites will be measured in the rest frame of the jet. If not distinguished explicitly the term 'electron' may include positrons as well.

The total energy density $U_{\rm jet}$ in the jet is the sum of magnetic field energy density $U_{\rm B} = B^2/8\pi$, turbulent kinetic plasma energy density $U_{\rm turb} \simeq U_{\rm B}$ assumed to be in equipartition with the magnetic field and the energy density of relativistic particles $U_{\rm e+p} = k_{\rm e+p}U_{\rm B}$.

$$U_{\rm jet} = U_{\rm B} + U_{\rm turb} + U_{\rm e+p} = u_{\rm j_o} B^2/8\pi \tag{5}$$

$$u_{\rm j_o} \simeq (2 + k_{\rm e+p}) \tag{6}$$

As $k_{\rm e+p}$ can have any value we also allow discussion of non-equipartition situations and especially any small value $k_{\rm e+p} \ll 1$ where the plasma is dominated by the magnetic field. Nevertheless, we will refer to this equation as the equipartition assumption.

The number densities of relativistic particles in the jet are described by a power law distribution of the form

$$dN_{\rm e|p} = K_{\rm e|p}\, \gamma_{\rm e|p}^{-p}\, d\gamma \tag{7}$$

where $\gamma_{\rm e|p}$ is the Lorentz factor of electrons and protons respectively. For simplicity we will assume, that the exponent p is the same for both species. The constants $K_{\rm e|p}$ can be evaluated with help of Eq.(5), where we assume that the particles are within a factor $k_{\rm e+p}$ in equilibrium with the magnetic energy density.

$$k_{\rm e+p}\frac{B^2}{8\pi} = K_{\rm e}\int_{\gamma_{\rm min,e}}^{\gamma_{\rm max,e}} \gamma m_{\rm e} c^2 \gamma^{-p} d\gamma + K_{\rm p}\int_{\gamma_{\rm min,p}}^{\gamma_{\rm max,p}} \gamma m_{\rm p} c^2 \gamma^{-p} d\gamma \tag{8}$$

$$\Rightarrow K_{\rm e} = B^2/\left(8\pi f m_{\rm e} c^2\right) \tag{9}$$

where we have defined the integration factors $\Lambda_{\rm e}$ and $\Lambda_{\rm p}$ as

$$\Lambda_{\rm e|p} = \begin{cases} \left(\gamma_{{\rm min},e|p}^{2-p} - \gamma_{{\rm max},e|p}^{2-p}\right)/(p-2) & : \quad p \neq 2 \\ \ln \gamma_{{\rm max},e|p}/\gamma_{{\rm min},e|p} & : \quad p = 2 \end{cases}, \tag{10}$$

the relativistic p/e ratio (plus one)

$$\mu_{\rm p/e} = \left(1 + \frac{K_{\rm p}\Lambda_{\rm p} m_{\rm p}}{K_{\rm e}\Lambda_{\rm e} m_{\rm e}}\right) \tag{11}$$

and a fudgefactor

$$f = \Lambda_{\rm e}\mu_{\rm p/e}/k_{\rm e+p}. \tag{12}$$

To ease understanding, we will discuss meaning, limits and expected values of our parameters in a special subsection (2.5).

Having the normalization specified it is now straightforward to integrate the powerlaw Eq.(7) and obtain the total number density of relativistic electrons and protons.

$$n_{\rm e} = B^2/\left(8\pi\gamma_{\rm min,e}^{p-1} f m_{\rm e} c^2 (p-1)\right), \tag{13}$$

$$n_{\rm p} = (\mu_{\rm p/e} - 1)\gamma_{\rm min,e}^{p-1} n_{\rm e}\frac{\Lambda_{\rm e} m_{\rm e}}{\Lambda_{\rm p} m_{\rm p}}. \tag{14}$$

For small $\mu_{\rm p/e}$ the number of relativistic protons will be negligible compared to the number of either relativistic electrons or thermal protons, whereas the fraction $x_{\rm e} = n_{\rm e}/n_{\rm tot}$ of relativistic electron density $n_{\rm e}$ compared to the total number density of protons $n_{\rm tot}$ (relativistic + thermal protons) might be fairly high. For simplicity we define a modified electron ratio

$$x'_{\rm e} = x_{\rm e}\gamma_{\rm min,e}^{p-1}. \tag{15}$$

and obtain as total density from Eq.(13)

$$n_{\rm tot} = B^2/\left(8\pi x'_{\rm e} f m_{\rm e} c^2 (p-1)\right). \tag{16}$$

Considering the disk in-flow as primary source for mass out-flow, the values for density and magnetic field are not arbitrary but are fixed by the jet parameters, i.e. the proper velocity $\gamma_{\rm j}\beta_{\rm j}$, the width of the nozzle $r_{\rm nozz}$ and the mass loss rate of the jet $\dot{M}_{\rm jet}$ which in turn is constrained by the maximum mass supply from the disk.

$$\dot{M}_{\rm jet} = q_{\rm m}\dot{M}_{\rm disk} = \gamma_{\rm j}\beta_{\rm j} c n_{\rm tot} m_{\rm p} \pi \left(r_{\rm nozz} R_{\rm g}\right)^2 \tag{17}$$

By comparing the number density following from this equation

$$n_{\rm tot} = 5.5 \cdot 10^{10}{\rm cm}^{-3} \left(\frac{q_{\rm m}}{0.03}\right) \frac{\dot{m}_{\rm disk}}{\gamma_{\rm j}\beta_{\rm j} m_8^2 r_{\rm nozz}^2} \tag{18}$$

with the number density needed to establish equipartition between magnetic field and relativistic particles (Eq. 16) we can express the magnetic field in terms of the dimensionless parameters described above.

$$B_{\rm nozz} = 1064\,{\rm G}\sqrt{\frac{f x_{\rm e}'(p-1)}{\gamma_{\rm j}\beta_{\rm j} r_{\rm nozz}^2} \frac{\dot{m}_{\rm disk}}{m_8^2} \left(\frac{q_{\rm m}}{0.03}\right)} \tag{19}$$

With this information at hand we can fix the initial conditions in the plasma flow under the additional assumption that the magnetic field can be included in the overall equation of state of a perfect gas with pressure

$$P_{\rm jet} = (\Gamma - 1) U_{\rm jet} = u_{\rm j_0}(\Gamma - 1) B^2/8\pi. \tag{20}$$

A turbulent and almost isotropic magnetic field gas has the ratio 1/3 between pressure and energy density ($\Gamma = 4/3$). For an ordered magnetic field (e.g. a toroidal component only) this ratio would be unity. In the following we give some basic equations for the plasma, following the description developed by Königl (1980).

The enthalpy density plus rest mass energy of the plasma for a constant adiabatic index Γ is

$$\omega = m_{\rm p} n_{\rm tot} c^2 + \Gamma P_{\rm jet}/(\Gamma - 1); \tag{21}$$

pressure and enthalpy combined tell us the local sound speed of the plasma in its local rest frame

$$\beta_{\rm s} = \sqrt{\Gamma P/\omega} \tag{22}$$

$$\simeq \min\left(\sqrt{u_{\rm j_0}(\Gamma^2 - \Gamma) f x_{\rm e}'(p-1) m_{\rm e}/m_{\rm p}}, \beta_{\rm s,max}\right) \tag{23}$$

where the maximum sound speed is

$$\beta_{\rm s,max} = \sqrt{\Gamma - 1}. \tag{24}$$

For usual adiabatic indices the latter will be well below 1, so that it is fairly safe to assume $\gamma_{\rm s} = 1/\sqrt{1-\beta_{\rm s}^2} \approx 1$. In this case we can write the relativistic Mach number of the flow as

$$\mathcal{M} = \gamma_{\rm j}\beta_{\rm j}/\beta_{\rm s} \tag{25}$$

which gives the ratio between the proper flow speed and the internal sound speed. One consequence of relativistic gas dynamics and the upper limit for the sound speed is that any flow with bulk relativistic motion is supersonic and needs no collimation. For a free plasma stream the Mach number defines the semi-opening angle unless we have a situation where the field lines are arranged such that they confine the flow. Such a confinement is more likely to happen in the nozzle region and in the following we will ignore this possibility, rather take the photon gas approximation and set the adiabatic index of the plasma flow to

$$\Gamma = 4/3. \tag{26}$$

The underlying picture is a turbulent magnetic field in the inner jet cone. However, the whole description remains valid, if one considers an ordered magnetic field. In case of a solely toroidal magnetic field only a few factors will change slightly but the vertical ($1/z$, see below) dependence of B will be the same as in the turbulent case. Only for a predominantly poloidal magnetic field, we will get a different (steeper) z depependence of B. Polarizaton measurement do show different orientations of the magnetic field along the jets, suggesting different orientations of a net magnetic field as well (sometimes poloidal, sometimes toroidal). This is not a problem as long as the turbulent component of the magnetic field dominates the internal energy, otherwise some of our conclusions could change.

2.3. Energy equation

We now investigate the energy demand of the jet as described above. The energy equation describing our jet-disk system is simply the relativistic Bernoulli equation.

$$\gamma_{\rm j}\omega/n_{\rm tot} = \omega/n_{\rm tot}|_\infty \tag{27}$$

The values on the left hand side depend on the quantities $q_{\rm m}$ and $\beta_{\rm s}$ and the right hand side is determined by the energy supply from the accretion process and is parametrized by $q_{\rm j}$. After some algebraic transformations we find

$$\gamma_{\rm j} q_{\rm m}\left(1 + \frac{\beta_{\rm s}^2}{\Gamma - 1}\right) = q_{\rm j}. \tag{28}$$

If we subtract the rest mass energy from both sides and take the non-relativistic limit, this equation simply states that the total power in the jet consists of the power in relativistic particles and the magnetic field (internal power) plus the kinetic energy of the matter (kinetic power).

In case the internal sound speed reaches its maximum $\beta_{\rm s} = \sqrt{\Gamma - 1}$ the bracket evaluates to 2 and the internal power equals the kinetic power of the jet

$$2\gamma_{\rm j} q_{\rm m} = q_{\rm j} \quad \Rightarrow \quad q_{\rm m} = \frac{q_{\rm j}}{2\gamma_{\rm j} q_{\rm l}} \frac{L_{\rm disk}}{\dot{M}_{\rm disk} c^2}. \tag{29}$$

In most other cases ($\mathcal{M} \gg \gamma_{\rm j}\beta_{\rm j}/\sqrt{\Gamma - 1}$) we may use the approximation

$$\gamma_{\rm j} q_{\rm m} \simeq q_{\rm j} \quad \Rightarrow \quad q_{\rm m} = \frac{q_{\rm j}}{\gamma_{\rm j} q_{\rm l}} \frac{L_{\rm disk}}{\dot{M}_{\rm disk} c^2}. \tag{30}$$

2.4. Maximal jets

Obviously this energy equation limits the internal power to a maximum, which is set by the kinetic power (both in the observers frame). The case $\beta_s = \beta_{s,\max}$ is the most extreme case in any model. Equation (29) transformed into the restframe of the gas tells us that in a given volume the enthalpy equals the rest mass energy of the protons – which is the microscopic equivalent to the statement that bulk kinetic power equals bulk internal power. We therefore will refer to this case as the 'maximal case' or the 'maximal jet'. Usually the kinetic power dominates the total energy but as soon as the magnetic field contributes a significant fraction to the total jet power, energy conservation provides us with a strict upper limit for the maximal magnetic field. Increasing the internal power would then increase the total power as well beyond the value $Q_{\rm jet}$ assigned to the jet. Even by dropping the assumption of a 'heavy' jet and taking out the protons from the energy balance (decreasing the kinetic power) we would gain only a negligible factor $\sqrt{2}$ for the magnetic field.

We have to make sure that this limit is not violated and formulate it as an additional condition for the plasma parameters involved. The total energy flow

$$\mathrm{EF} = \gamma_{\rm j}^2 \beta_{\rm j} c \omega \pi (r R_{\rm g})^2 \leq q_{\rm j} Q_{\rm accr} \tag{31}$$

is smaller or equal the total jet power, which leads to

$$\mu_{\rm p/e} \leq 100 \frac{k_{\rm e+p}}{\ln\left(\frac{\gamma_{\rm max,e}}{\gamma_{\rm min,e}}\frac{1}{100}\right) u_3 \gamma_{\rm min,e} x_{\rm e}} \tag{32}$$

We can turn this argument around and ask, what combination of parameters always gives the equality between internal and kinetic power, i.e. a maximal jet, and find

$$\mu_{\rm p/e} = 1.0 \frac{k_{\rm e+p}}{\ln\left(\frac{\gamma_{\rm max,e}}{\gamma_{\rm min,e}}\frac{1}{100}\right) u_3 \gamma_{\rm e,100} x_{\rm e}} \tag{33}$$

Equation (33) will be used to eliminate the proton/electron ratio in all subsequent equations for maximal jets. We will mark these equations with an asterisk ensuring that whatever parameters are used one still has a maximal jet.

$$^* = \text{“maximal case''} \tag{34}$$

2.5. Discussion of parameters

In this subsection we discuss the parameters which we introduced and their expected values and limitations.

- $r_{\rm nozz}$ is the radius of the jet at the disk/jet interface divided by the gravitational radius. It can have any value larger or equal the inner radius of the disk, which for a maximally rotating black hole is $\simeq 1.23$ and likely values are $\gtrsim 2$ where the disk structure equations do have a maximum and the boundary layer begins, but could also be somewhat higher if one considers a rapidly rotating magnetosphere of the disk (Camenzind 1986, also Sec. 4).
- $x_{\rm e}$ is the ratio of relativistic electron density $n_{\rm e}$ to the total number density of protons $n_{\rm tot}$(*relativistic+thermal*). If charge neutrality is assumed and no pair creation takes place than $x_{\rm e} \leq 1$ is a strict limit. Reaching the upper limit would mean all thermal electrons are accelerated. It is doubtful if any process can be so efficient and usually $x_{\rm e} = 0.1-0.5$ is already considered an extreme limit. In cases where pair creation is possible $x_{\rm e}$ could higher than 1 but energy conservation (Eq. 32, $\mu_{\rm p/e} \geq 1$ and $\gamma_{\rm min,e} \geq 1$ per definition!) demands $x_{\rm e} \leq 100\, k_{\rm e+p}/\ln\left(\frac{\gamma_{\rm max,e}}{\gamma_{\rm min,e}}\frac{1}{100}\right) u_3 \gamma_{\rm min,e}$.
- $\gamma_{\rm min,e}$ is the minimum Lorentz factor of the relativistic electron population. As a powerlaw with low energy cut-off is only a first order approximation this could have several meanings: a simple break in the energy spectrum of the electrons with a much flatter slope than $p = 2$ below $\gamma_{\rm min,e}$, a thermal distribution with high temperatures ($T = \gamma_{\rm min,e} 6 \cdot 10^9$ K) plus powerlaw or a real cut-off towards low energies caused by a threshold condition in the acceleration process. The only limit is $\gamma_{\rm min,e} > 1$. For energies higher than a critical value ($\gamma_{\rm min,e} \gtrsim 100$) the electron fraction $x_{\rm e}$ has to decrease (Eq. 32) simultaneously. We emphasize that $\gamma_{\rm min,e} \gtrsim 100$ is a necessary consequence of the pion decay following hadronic interactions (Biermann et al., in prep.).
- $x_{\rm e}'$ is defined as $\gamma_{\rm min,e}^{(p-1)} x_{\rm e}$ and is a normalized and dimensionless measure for the energy density of the relativistic electrons if $p = 2$. Again Eq.(32) limits $x_{\rm e}'$ to be $\lesssim 100$.
- $\mu_{\rm p/e}$ is the cosmic ray proton/electron ratio plus one. The cosmic ray ratio is the ratio of the energy densities in relativistic protons and electrons integrated from $\gamma_{\rm min,p} = 1$ and $\gamma_{\rm min,e}$ respectively to infinity. By definition this value must be larger than unity. Exactly unity means there are no protons a all. Values discussed in the literature usually range from a few to 100 in the cosmic rays themselves and 2000 for certain acceleration theories. If the electron population is a product of hadronic interactions (secondary pairs) than one naively would expect that on average the electrons should not gain more power than the protons, i.e. $\mu_{\rm p/e} \gtrsim 2$.
- $k_{\rm e+p}$ is the equipartition parameter. $k_{\rm e+p} = 1$ means: the energy density of the magnetic field equals exactly the energy density of all relativistic particles (electrons + protons). $k_{\rm e+p} \gg 1$ would imply that electrons and protons have gained much more energy than is stored in the magnetic field. With regard to the fact that all likely acceleration mechanisms require a strong magnetic field, we consider this possibility un-

likely and usually assumed values are in the range $k_{\rm e+p} \sim 0.01 - 1$.

- f is defined as $\Lambda_{\rm e}\mu_{\rm p/e}/k_{\rm e+p}$ and needed in the non-maximal case as an additional parameter to describe the relative strength of the magnetic field energy density to the relativistic electron density. If one excludes $k_{\rm e+p} \gg 1$ (see above) and takes $\gamma_{\rm max,e}/\gamma_{\rm min,e} \simeq 100$ we have $f \gtrsim 4$ for $p = 2$, whereas if $p = 3$ we have $f \gtrsim \gamma_{\rm min,e}^{-1}$.

To shorten the equations we will also make use of the following definitions and standard parameters whose values are discussed in more detail in Paper II.

- The ratio $Q_{\rm jet}/L_{\rm disk}$ between total jet power and disk luminosity
$$q_{\rm j/l} := q_{\rm j}/q_{\rm l} = Q_{\rm jet}/L_{\rm disk} \qquad (35)$$
which can have any value between zero (no jet) and infinity (no disk) , but we consider $q_{\rm j/l} \lesssim 1$ as a sensible limit.
- The disk luminosity, which for a 'typical' AGN is in the range $10^{44} - 10^{48}$ erg/sec.
$$L_{46} := L_{\rm disk}/\left(10^{46}{\rm erg/sec}\right). \qquad (36)$$
- The jet velocity and its bulk Lorentz factor $\gamma_{\rm j}$ usually assumed to be in the range $\gamma_{\rm j} \simeq 2 - 20$ (Ghisellini et al. 1993).
$$\gamma_{\rm j,5} := \gamma_{\rm j}/5 \qquad (37)$$
The bulk Lorentz factor (jet velocity) has a more subtle limit. In order to still have a jet and not a quasi spherical wind the Mach number should be larger than unity. For a maximal jet we need $\beta_{\rm j}\gamma_{\rm j} > 0.58$ and for lower bulk velocities $\beta_{\rm s}$ (i.e. f or $x_{\rm e}'$) also has to be lowered and one rather should use the Mach number as a parameter for sub-relativistic jets.
- The minimum (break) Lorentz factor of the electron distribution, which may be in some cases ≥ 100 (see Discussion).
$$\gamma_{e,100} := \gamma_{\rm min,e}/100 \qquad (38)$$
- Likewise, the modified electron density
$$x_{\rm e,100}' := \gamma_{\rm e,100}^{p-1} x_{\rm e} \qquad (39)$$
where one has to be careful if $p \neq 2$ as then because of the non-linearity in $\gamma_{\rm e,100}^{p-1}$ we have $x_{\rm e,100}' \neq x_{\rm e}'/100$.
- The ratio $u_{\rm j_o}$ between total energy density in the jet and the magnetic energy density. In case we have equipartition between turbulent kinetic energy, magnetic field and relativistic particles this value is 3, neglecting turbulence gives 2 (or $1 + k_{\rm e+p}$). For high values of $k_{\rm e+p}$ this factor is no longer a small number and $u_{\rm j_o} \propto k_{\rm e+p}$.
$$u_3 := u_{\rm j_o}/3 = (2 + k_{\rm e+p})/3 \qquad (40)$$

Our general conclusions are qualitatively independent of the power law index p. For the observational consequences we concentrate on the canonical case $p = 2$ and give some equations for $p = 2.5$ in the Appendix.

Finally there is another limit we have to check. For the electrons one still could argue that they actually are pairs and therefore the electron fraction $x_{\rm e}$ may exceed unity, for protons the fraction $x_{\rm p}$ of relativistic protons in the jet must be less or equal unity otherwise mass conservation is violated. From Eqs.(14,18,19) we find that
$$x_{\rm p} = 5.4 \cdot 10^{-4}\, \gamma_{{\rm min},e} x_{\rm e} \frac{\Lambda_e}{\Lambda_{\rm p}} \left(\mu_{\rm p/e} - 1\right) \leq 1. \qquad (41)$$
Usually this limit is not important but in the maximal case where $\gamma_{\rm min} \gtrsim 100$ this equation limits the proton/electron ratio $\mu_{p/e}$ to be $\lesssim 100$. Fortunately, this limit is automatically met by virtue of Eq.(33), because for $k_{\rm e+p} \gg 1$ we have $u_3 = k_{\rm e+p}$ and a high value of $\mu_{\rm p/e} \gg 1$ can not be obtained while keeping $x_{\rm e}'$ constant at $\gtrsim 100$.

3. Observational consequences

3.1. The cone

Beyond the nozzle the flow will expand sideways; either the jet has still a lot of angular momentum from the disk leading to an opening of the streamlines, or the strong and turbulent magnetic field dominates the internal pressure and leads to an expansion of the jet. In the latter case the semi-opening angle of the flow[1] ϕ is simply given by the relativistic Mach number $\mathcal{M}$ (Königl 1980). If, in the other case, the opening angle is given by the angular momentum, then the opening angle should be larger than this and we have
$$\phi \geq \arcsin \mathcal{M}^{-1}. \qquad (42)$$
We will use only the equality
$$\phi \simeq 0.3^\circ \cdot \sqrt{\frac{f u_3 x_{\rm e}'}{\beta_{\rm j}^2 \gamma_{\rm j,5}^2}} \qquad (43)$$
$$\phi^* = 6.6^\circ \cdot \left(\beta_{\rm j}\gamma_{\rm j,5}\right)^{-1} \qquad (44)$$
but one has to bear in mind that a larger opening angle will later reduce the radiative efficiency of the jet and in the final analysis therefore increase the energy demand of the jet relative to the disk. The cylinder-symmetrical shape $r(z)$ of the cone is given by
$$r_{\rm jet}(z_{\rm jet}) = r_{\rm nozz} + (z_{\rm jet} - z_{\rm nozz})/\mathcal{M} \overset{z\to\infty}{=} z_{\rm jet}/\mathcal{M}. \qquad (45)$$
Considering an adiabatic jet, all quantities derived in the previous section will follow the laws of adiabatic expansion; we only have to substitute the radius r by means of the above equation (45) and obtain the hydrodynamical quantities as functions of the distance z from the disk. The magnetic field declines with
$$B = B_{\rm nozz} r_{\rm j}(z)^{-\aleph}. \qquad (46)$$

[1] This is defined to reflect the scale of the cone radius and is not identical with the opening angle as defined in some hydrodynamical simulations where zero pressure is reached.

Conservation of magnetic energy leads to $\aleph = 1$ (the familiar $B_{\rm j} \propto 1/z_{\rm jet}$ decline) and a constant Mach number because particle and energy density both scale with $1/z_{\rm jet}^2$.

Note that there is no ad-hoc need for reacceleration of the relativistic particles. Likewise there is no dissipation or recreation of the magnetic field in the case $\aleph = 1$; but from synchrotron energy loss arguments we will find that acceleration of relativistic particles in the jet itself indeed is necessary. Nevertheless, our description will still be correct if this acceleration always leads to (quasi-)equipartition with the magnetic field.

We also note, that shocks will increase the magnetic field strength, taking the energy from the overall flow. Thus, in the case of semi-periodic shock structures, it is quite conceivable, that an average equilibrium between energetic particles, magnetic field energy and flow energy can be maintained. The high amount of energy in relativistic particles we need for some models is not unusual within the general picture of shock acceleration (see Drury 1983).

3.2. Emission from the radio core

Now we calculate the synchrotron emission of the different parts of the jet. First, we give the emission and absorption coefficients for powerlaw distributions of relativistic electrons (see Eq. 7) with index $p = 2$ in the rest frame. For the pitch angle of the electrons $\alpha_{\rm pitch}$ we took the values which inserted into the formulae yield the average for an isotropic turbulent medium. From (Rybicki & Lightman 1979) we then get

$$\epsilon_{\rm sync} = 5.5 \cdot 10^{-19} \frac{\rm erg}{\rm s\,cm^3\,Hz} f^{-1} \left(\frac{B}{\rm G}\right)^{3.5} \left(\frac{\nu}{\rm GHz}\right)^{-.5} \tag{47}$$

$$\alpha_{(\rm pitch,\epsilon)} = 53.4^\circ \tag{48}$$

$$\kappa_{\rm sync} = 4.5 \cdot 10^{-12}\,{\rm cm}^{-1} f^{-1} \left(\frac{B}{\rm G}\right)^{4} \left(\frac{\nu}{\rm GHz}\right)^{-3} \tag{49}$$

$$\alpha_{(\rm pitch,\kappa)} = 54.7^\circ. \tag{50}$$

In Sec. 2 and the beginning of this section we defined the state of the emitting plasma in the freely expanding inner jet cone beyond the nozzle as a function of several dimensionless parameters. Using the synchrotron emissivity we can now calculate the total synchrotron emission from that region. The optical depth τ for a ray right through the central axis of the cone is given by

$$\tau = 2 r_{\rm j} R_{\rm g} \kappa_{\rm sync} / \sin i \tag{51}$$

using Eq.(45) to express the shape of the cone. From the condition $\tau = 1$ we find the part of the jet, where for an observed[2] frequency $\nu_{\rm s,obs}$ the jet becomes synchrotron self absorbed.

[2] This means a frequency observed in the rest frame of the *quasar*, and does not include cosmological corrections.

$$Z_{\rm ssa} = 19\,{\rm pc}\, \frac{x_{\rm e}^{\frac{1}{6}} \beta_{\rm j}^{\frac{1}{3}}}{u_3^{\frac{1}{3}} \gamma_{\rm j,5}^{\frac{1}{3}} f^{\frac{1}{6}} \sin i^{\frac{1}{3}}} \frac{\rm GHz}{\nu_{\rm s,obs}/\mathcal{D}} \left(q_{\rm j/l} L_{46}\right)^{\frac{2}{3}} \tag{52}$$

$$Z^*_{\rm ssa} = 31\,{\rm pc} \left(\frac{x'_{\rm e,100} \beta_{\rm j}}{\gamma_{\rm j,5} u_3 \sin i}\right)^{\frac{1}{3}} \frac{\rm GHz}{\nu_{\rm s,obs}/\mathcal{D}} \left(q_{\rm j/l} L_{46}\right)^{\frac{2}{3}} \tag{53}$$

The size of the visible inner jet cone scales proportionally with the wavelength and the typical size of the inner jet is for AGN on the parsec scale. The size seen by an observer has to be multiplied with an additional factor $\sin i$. We can now integrate the emission of the cone from $Z_{\rm ssa}$ to infinity in the rest frame of the jet

$$L_{\nu_{\rm s}} = 4\pi \int_{Z_{\rm ssa}}^{\infty} \epsilon_{\rm sync} \pi r_{\rm j}^2 (z_{\rm jet}) dz_{\rm jet} \tag{54}$$

yielding the total monochromatic luminosity of one jet cone in the rest frame. To get the observed fluxes we have to perform the transformations (Lind & Blandford 1985)

$$\mathcal{D} = 1/\gamma_{\rm j}(1 - \beta_{\rm j} \cos i_{\rm obs}), \quad L_{\nu,{\rm obs}}(\nu_{\rm obs}) = \mathcal{D}^2 L_\nu(\nu_{\rm obs}/\mathcal{D})$$
$$\nu_{\rm s} = \nu_{\rm s,obs}/\mathcal{D}, \quad \sin i = \mathcal{D} \sin i_{\rm obs}. \tag{55}$$

Thus we have

$$L_{\nu_{\rm s,obs}} = 4.5 \cdot 10^{31} \frac{\rm erg}{\rm s\,Hz} \left(q_{\rm j/l} L_{46}\right)^{\frac{17}{12}} \cdot \frac{\mathcal{D}^{\frac{13}{6}} \sin i_{\rm obs}^{\frac{1}{6}} f^{\frac{1}{12}} x_{\rm e}'^{\frac{11}{12}}}{\sqrt{u_3} \gamma_{\rm j,5}^{\frac{11}{6}} \beta_{\rm j}^{\frac{5}{12}}} \tag{56}$$

$$L^*_{\nu_{\rm s,obs}} = 1.3 \cdot 10^{33} \frac{\rm erg}{\rm s\,Hz} \left(q_{\rm j/l} L_{46}\right)^{\frac{17}{12}} \cdot \frac{\mathcal{D}^{\frac{13}{6}} \sin i_{\rm obs}^{\frac{1}{6}} x_{\rm e,100}'^{\frac{5}{6}}}{\gamma_{\rm j,5}^{\frac{11}{6}} \beta_{\rm j}^{\frac{5}{12}} u_3^{\frac{7}{12}}} \tag{57}$$

Obviously the frequency cancels out in this equation (for all values of p) and the resulting spectrum of the cone is flat up to a maximum frequency (see below). The typical luminosity for cores of radio loud quasars with a disk luminosity of 10^{46} erg/sec is in the range $2 \cdot 10^{31} - 6 \cdot 10^{32}$ erg/sec/Hz at 5 GHz (e.g. Paper II). To avoid extreme parameters ($q_{\rm j/l} \gg 1$) one is forced to choose a model close to the maximal case (Eq. 57) in order to reproduce these high luminosities. A moderate value $q_{\rm j/l} \approx 0.3$ seems to be sufficient in the maximal case.

Moreover, it is quite interesting that the flux emitted from the jet cone need not scale linearly with the accretion rate. This is a consequence of the nonlinearity between the magnetic energy density ($\propto B^2 \propto \dot{m}$) and the synchrotron emissivity ($\propto B^{3.5}$). Because of jet geometry and self-absorption this also depends slightly on the electron powerlaw. For very large p (approaching a monoenergetic distribution) radio emission and disk luminosity become proportional.

As noted before (Ghisellini et al. 1993) the brightness temperature of the cone (in the rest frame of the jet!)

$$T_{\rm b} \;=\; 1\cdot 10^{11}\,{\rm K}\left(\frac{x'_{\rm e} q_{\rm j/d} L_{46}}{f\gamma_{\rm j,5}^2\beta_{\rm j}}\right)^{\frac{1}{12}} \sin i^{\frac{5}{6}} \qquad (58)$$

$$T_{\rm b}^* \;=\; 1.2\cdot 10^{11}\,{\rm K}\left(\frac{{x'_{\rm e,100}}^2 u_3 q_{\rm j/l} L_{46}}{\gamma_{\rm j,5}^2\beta_{\rm j}}\right)^{\frac{1}{12}} \sin i^{\frac{5}{6}} \qquad (59)$$

is constant along the jet axis and depends very weakly on the parameters. The numbers may change between 10^{11} Kelvin for $p=2$ and 10^{10} Kelvin for $p=3$. The observational finding that there is a maximum brightness temperature of $T_{\rm b}\lesssim 10^{12}$Kelvin (Kellermann & Pauliny-Toth 1969) might therefore not only be due to the synchrotron self-compton limit but is a natural consequence of an adiabatic jet in a Mach cone. This is strongly supported by more recent investigations by Ghisellini et al. 1993, where it is found that the brightness temperature in the rest frame of VLBI jets has an extremely narrow distribution around $1.8\cdot 10^{11}$Kelvin – pointing nearer to $p=2$ in our model.

3.3. High frequency cut-off and maximum Lorentz factors

Until now we have treated the jet as being an adiabatically expanding flow and neglected all radiation losses. However, energy conservation forces us to make sure that the energy loss by synchrotron radiation ($L_{\rm jet}=\int_0^{\nu_{\rm max}} L_{\nu_{\rm s}} d\nu$) does not exceed a certain fraction

$$\eta_{\rm sync} = L_{\rm jet}/\left(\gamma_{\rm j}^2\beta_{\rm j} c\pi\left(r_{\rm nozz}R_{\rm g}\right)^2\Gamma P_{\rm jet}/\left(\Gamma-1\right)\right) \qquad (60)$$

of the internal energy flow. For reference we deliberately take a maximum efficiency of 33% for the conversion of internal energy into radiation and define $\eta_{\rm sync}=1/3\cdot\eta_{\frac{1}{3}}$. Integration of the flat spectrum Eq.(56) in the rest frame yields a maximum frequency $\nu_{\rm max}$ where the spectrum has to cut off (or steepen substantially) to fulfill this limitation (here we ignore the anisotropy of the radiation field).

$$\nu_{\rm max,1} \;=\; 160\,{\rm GHz}\,\mathcal{D}\eta_{1/3}\frac{f^{\frac{11}{12}}\gamma_{\rm j,5}^{\frac{11}{6}}\beta_{\rm j}^{\frac{5}{12}}{x'_{\rm e}}^{\frac{1}{12}}u_3^{\frac{3}{2}}}{\left(q_{\rm j/l}L_{46}\right)^{\frac{5}{12}}\sin i^{\frac{1}{6}}} \qquad (61)$$

$$\nu_{\rm max,1}^* \;=\; 1300\,{\rm GHz}\,\mathcal{D}\eta_{1/3}\frac{\gamma_{\rm j,5}^{\frac{5}{6}}\beta_{\rm j}^{\frac{5}{12}}u_3^{\frac{7}{12}}}{{x'_{\rm e,100}}^{\frac{5}{6}}\left(q_{\rm j/l}L_{46}\right)^{\frac{5}{12}}\sin i^{\frac{1}{6}}} \qquad (62)$$

And indeed such a break is observed (Chini et al. 89b), where from 1.3 and 0.8 mm fluxes one can imply a turnover of the core spectrum. A more precise determination of the break frequency would be an interesting test for this models. Because $\nu_{\rm max}$ is a function of the Doppler factor, the observed break frequency is smaller for radio galaxies (anti-boosted) than for Blazars (boosted) if the unified scheme is correct.

In AGN this maximum frequency is much lower than the characteristic frequency in the very inner parts of the jet obtained by extrapolating this theory down to the nozzle. Hence we have to limit the maximum Lorentz factor of the electrons in the nozzle to prevent the jet from exhausting itself in the very beginning. The characteristic frequency of an electron with energy $\gamma_{\rm e} m_{\rm e} c^2$ in an magnetic field B is given by

$$\nu_{\rm e} = 4.2\cdot 10^6\,{\rm Hz}\;\left(B/{\rm Gauss}\right)\gamma_{\rm e}^2 \qquad (63)$$

and we can equate $\nu_{\rm max}$ with $\nu_{\rm e}$ using the magnetic field of the nozzle Eq.(19) to obtain the maximal initial Lorentz factor for the electrons in the jet

$$\gamma_{\rm nozz,max} \;=\; 9\,\frac{\sqrt{\eta_{03}m_8 r_{\rm nozz}}\beta_{\rm j}^{\frac{11}{24}}\gamma_{\rm j,5}^{\frac{17}{12}}u_3^{\frac{3}{4}}}{{x'_{\rm e}}^{\frac{5}{24}}\left(q_{\rm j/l}L_{46}\right)^{\frac{11}{24}}\sin i^{\frac{1}{12}}} \qquad (64)$$

$$\gamma_{\rm nozz,max}^* \;=\; 6\,\frac{\sqrt{\eta_{03}m_8 r_{\rm nozz}}\beta_{\rm j}^{\frac{11}{24}}\gamma_{\rm j,5}^{\frac{17}{12}}u_3^{\frac{13}{24}}}{{x'_{\rm e,100}}^{\frac{5}{12}}\left(q_{\rm j/l}L_{46}\right)^{\frac{11}{24}}\sin i^{\frac{1}{12}}} \qquad (65)$$

For the maximal case this limit is inconsistent with a low energy cut-off at $\gamma_{\rm e}=100$. Unless pairs with $\gamma_{\rm min}\simeq 1$ are present, in situ acceleration of electrons is therefore necessary and the high internal energy flow in the beginning is only due to a Poynting flux with an electron distribution not in equipartition with the magnetic field and starting at low energies (model **B0** & **Bp** see Discussion). As we have not considered the effects of self-absorption (but see next section) and the turn over of the spectrum, slightly higher Lorentz factors are possible, but if they are initially much higher than these the jet would be completely dissipated by radiation losses. Starting with low Lorentz factors and shuffling the electrons towards higher energies by reacceleration in the jet into a state of equilibrium without severe radiation losses is possible only far away from the black hole and this scale is approximately given by the distance

$$Z_{\rm min,1}^* = 5\cdot 10^{16}\,{\rm cm}\,\frac{\left(q_{\rm j/l}L_{46}\right)^{\frac{13}{12}}x_{\rm e,100}^{\frac{7}{6}}}{\eta_{03}\beta_{\rm j}^{\frac{1}{12}}\gamma_{\rm j,5}^{\frac{13}{6}}u_3^{\frac{11}{12}}\sin i^{\frac{1}{6}}} \qquad (66)$$

where the the high energy break $\nu_{\rm max,1}$ equals the peak (synchrotron self-absorption) frequency $\nu_{\rm s}$. This is the minimum scale for the beginning of the full jet emission. To ensure that the synchrotron emission in the optical thin part is not cut-off directly one also has to compare the synchrotron loss time $t_{\rm sync}=7.7\cdot 10^8\,{\rm sec}\;\left(\gamma_{\rm min,e}(B/{\rm Gauss})^2\right)^{-1}$ of the electrons with the time scale of the local adiabatic expansion $t_{\rm exp}=z_{\rm jet}R_{\rm g}/(\gamma_{\rm j}\beta_{\rm j}c)$. Beyond a distance

$$Z_{\rm min,2}^* = 8.6\cdot 10^{17}\,{\rm cm}\,\frac{q_{\rm j/l}L_{46}\gamma_{\rm min,100}}{\beta_{\rm j}\gamma_{\rm j,5}^2 u_3} \qquad (67)$$

the synchrotron spectrum can take its usual shape without severe radiation losses in the optically thin region around the synchrotron self absorption frequency. These scales are in agreement with the minimum size for the region where the γ-ray emission in blazars are proposed to originate (Dermer & Schlickeiser 1994, Mannheim 1993) suggesting a deeper connection between both processes. The frequency corresponding to this scale where a turnover of the flat spectrum is likely to occur is

$$\nu^*_{\rm max,2} = 70\,{\rm GHz}\;\mathcal{D}\left(\frac{\beta_{\rm j}\gamma_{\rm j}^2 u_3^2 x_{\rm e}}{\gamma^2_{100,{\rm e}} q_{\rm j/l} L_{46}\sin i}\right)^{\frac{1}{3}}. \tag{68}$$

This is a bit lower than $\nu^*_{\rm max,1}$ which is a strict upper limit for the break in the radio spectrum.

3.4. Self-absorption vs. optical thin turnover

The traditional picture to obtain the flat spectrum core is based on the overlap of self-absorbed synchrotron blobs. This, however, may be a critical assumption at least in the maximal case when one demands high minimum electron Lorentz factors. To check this, we have to compare the synchrotron self-absorption frequency derived in Eq.(52) with the characteristic frequency

$$\nu^*_{\rm c}(\gamma=\gamma_{\rm min,e}) = 14\,{\rm GHz}\;\gamma^2_{\rm min,100}\sqrt{\frac{\beta_{\rm j} q_{\rm j/l} L_{46}}{u_3}}\left(\frac{\rm pc}{Z_{\rm jet}}\right) \tag{69}$$

emitted by an electron with Lorentz factor $\gamma_{\rm min}$ in a maximal jet. The ratio between both frequencies

$$\frac{\nu^*_{\rm s}}{\nu^*_{\rm c}} = 1.45\,\gamma_{\rm min,100}^{-\frac{5}{3}}\left(\frac{q_{\rm j/l}L_{46}x_{\rm e}^2}{\beta_{\rm j}\gamma^2_{\rm j,5}\sin i^2}\right)^{\frac{1}{6}} \tag{70}$$

again is only a weak function of all parameters except $\gamma_{\rm min,e}$ and constant throughout the jet. In the non-maximal case this ratio is $\sim 10^4$ and negligible, but in the maximal case this is an important effect and almost impossible to avoid. It means that or $\gamma_{\rm min,e} > 120$ the spectrum will turn over already before synchrotron self-absorption sets in. One never gets a clear self absorbed $\nu^{2.5}$ spectrum but rather an optically thin $\nu^{\frac{1}{3}}$ spectrum which then turns over into a self-absobed 'thermal' ν^2 spectrum. The exact description will be given in a subsequent paper.

Fortunately both frequencies follow the same scaling along the jet and our calculations for the composite spectrum are still valid as the peaks at the two frequencies one integrates along the jet are very close. We still get a flat composite spectrum, not as an overlap of self-absorbed components but of components with an optically thin low energy turnover. This effect ensures that one always expects to see a flat to inverted spectrum. If for example one part of a variable and inhomogenous jet is enhanced and dominates the whole spectrum, we still will see a flat or even inverted spectrum at frequencies below $\nu_{\rm c}$. The spectrum of a resolved part of the jet core should be different as well; the low frequency turnover part of a VLBI blob will result in a spectrum possibly much flatter than the usual $\nu^{2.5}$.

3.5. Pair creation

Is the plasma in the jet optically thick, so that pair creation becomes important? To give an answer we calculate the optical depth $\tau_{\rm Th} = n\sigma_{\rm Th}2rR_{\rm g}$ of the jet for the Thomson cross section $\sigma_{\rm Th} = 6.65\cdot 10^{-25}{\rm cm}^2$

$$\tau_{\rm Th} \;=\; 50\,\frac{q_{\rm j/k}L_{46}}{\sqrt{fu_3}\gamma_{\rm j,5}m_8 z} \tag{71}$$

$$\tau^*_{\rm Th} \;=\; 1\,\frac{q_{\rm j/k}L_{46}}{\gamma_5 m_8 z} \tag{72}$$

and find that in all cases the jet is optically thin and $\tau_{\rm Th}$ decreases with distance. Only in the non-maximal case the very inner region of a few gravitational radii may be optically thick. The jet remains optically thin also for smaller black hole masses as than the luminosity decreases as well because of the Eddington limit.

One model very much under discussion to explain the hard X-ray spectrum of Seyfert galaxies and quasars is the idea, that there is a source of hard X-rays above the disk, which shines down on the disk. This hard radiation is then reprocessed in the disk, and reemitted with all the modifications due to interaction with the matter in the disk, thus yielding a number of spectral features, as observed. One mechanism to obtain this hard radiation is a pair creation cloud possibly connected to a putative jet. The primary source of energy could then be either a population of energetic electrons, or of energetic protons. In such models the pair creation opacity has to be fairly high to reprocess a large fraction of the primary energy (Zdziarski et al. 1990). In the context of our approach, we show here that this opacity is not high, and therefore that the notion of a pair creation cloud is not implied by our model.

3.6. Terminus

Now we leave the inner part of the jet and approach the same subject from the opposite side, namely the termination point. As magnetic field and particle densities expand adiabatically, the total energy density ED$=\gamma_{\rm j}^2\omega$ in the jet as measured in the lab-frame will decline in the same way as well all the way out to kpc-scales.

$$\begin{aligned}{\rm ED} \;&\simeq\; 8.4\cdot 10^{-7}\,\frac{\rm erg}{\rm cm^3}\left(\frac{\rm kpc}{Z_{\rm jet}}\right)^2 \\ &\cdot\frac{\beta_{\rm j}\gamma^2_{\rm j,5}\,(460+fu_3)\,q_{\rm j/l}L_{46}}{fx'_{\rm e}u_3}\end{aligned} \tag{73}$$

$${\rm ED}^* \;\simeq\; 8.4\cdot 10^{-7}\,\frac{\rm erg}{\rm cm^3}\left(\frac{\rm kpc}{Z_{\rm jet}}\right)^2\gamma^2_{\rm j,5}\beta_{\rm j}q_{\rm j/l}L_{46} \tag{74}$$

The non-maximal jet stores most of its energy in the kinetic energy of the plasma; together with the narrow beam this gives a ram pressure acting into the forward direction being a factor 500 higher than in the maximal case. Maximal jets have equal amounts of kinetic an internal energy, thus they will have a substantial amount of isotropic pressure. Taking only the amount of internal energy into account (dropping the factor 460 in Eq.(73)) we see that both types of jets have the same internal energy density due to a self regulating process: lowering the energy density will always lead to a smaller opening angle which in turn will increase the energy density again.

If we want to calculate the typical length scale of a jet, we have at least two possibilities for non-maximal jets. First one should simply compare the ram pressure of the jet beam ($P_{\rm ram} \simeq$ED) with the external pressure $P_{\rm ext}$, neglecting possible differences of the sound speeds in both media. For an external pressure of $P_{\rm ext} = P_{-12}10^{-12}{\rm erg/cm}^3$ we get a maximum scale length $Z_{\rm free}$ of the jet of

$$Z_{\rm free} = 20\,{\rm Mpc}\;\gamma_{\rm j,5}\sqrt{\frac{\beta_{\rm j} q_{\rm j/d} L_{46}}{f x_{\rm e}' u_3 P_{-12}}} \tag{75}$$

This of course would be deep inside the IGM with pressures much lower than 10^{-12} erg/cm^3 and hence there is little chance to stop such a jet at all. On the other hand the jet might be distorted much earlier as the cone has to be supported sideways against the external pressure as well. The scale where strong interactions between cone and external medium are expected then is given by the condition $P_{\rm ext} = 1/3ED^*$ for *both* types of jets (see above) leading to

$$Z^*_{\rm free} = 530\,{\rm kpc}\;\gamma_{\rm j,5}\sqrt{\beta_{\rm j} q_{\rm j/l} L_{46} P_{-12}^{-1}} \tag{76}$$

This can easily be matched with the parameter to the observed distances of lobes, which seem to cluster around ~ 300 kpc.

Of course there are quite a few processes which are able to decrease this size (e.g. mass entrainment). On the other hand, we see that in principle there is enough power stored in these jets to proceed far into the galaxy and even beyond. In the maximal case the agreement of theoretical interaction scale and observed lobe distances is reassuring, in the non-maximal case the situation is less clear as there are no observation to compare to. The jet is either so thin that it would 'cut' through the ISM and terminate far in the IGM (Eq. 75) or would be disrupted at the same distance as maximal jets (Eq. 76). For the inner jet cones we conclude that the energy density is always so high that no ISM is able to confine this part of the jet in any way and the assumption of a free jet is really justified.

These estimates also demonstrate that for higher ambient energy densities of the interstellar medium, such as observed in the Galactic Center region, or in the starburst galaxy M82, and low power jets these scales may decrease to galactic sizes. Thus there may be sources where the jet terminates inside the galaxy. Our picture is also invalid as soon as we leave the static situation and deal with young sources which still have to drill through the ISM. Here one should use the ram pressure for $P_{\rm ext}$ and by increasing this value by a factor $\sim 10^4$ one possibly could explain some of the compact steep spectrum sources (Fanti et al. 1990). In this context it would be interesting to analyze the low frequency turnover seen in this sources in light of the low-energy cut-off discussed here.

3.7. Lobes

What is the luminosity of the jet at the termination point? In this paper we do not intend to develop a new model for the emission of lobes and hotspots (see Meisenheimer 1992 for a review), but at least we have to check if in principle the jet is capable to transport the right portion of energy and magnetic fields outward so that it can supply extended structures like radio lobes of FR II type jets in radio loud quasars. The general numbers should not be completely incompatible with the usually inferred numbers for this regions.

We describe the terminal region as a cylinder where the jet is first slowed down to its internal sound speed and then terminates in a strong shock. We assume that the magnetic field in the first part is enhanced adiabatically by the slow down and then compressed by the shock with a compression ratio $v_1/v_2 = 7$ for $\Gamma = 4/3$. The magnetic field given by

$$B^*_{\rm lobe} = 7\cdot B_{\rm nozz}\frac{r_{\rm nozz}}{r_{\rm lobe}}\sqrt{\frac{\gamma_{\rm j}\beta_{\rm j}}{\beta_{\rm s}}} = 13\mu{\rm G}\,\sqrt{\frac{\beta_{\rm j} P_{-12}}{\gamma_{\rm j,5} u_3}} \tag{77}$$

is a bit lower than canonical values and independent of the accretion rate[3] and thus fairly constant, a finding which seems to be supported by observations (Meisenheimer 1992).

Radius and length of the cylindrical hotspot are given approximately by the radius of the jet cone before the termination point. For the distance from the core we take the value $Z^*_{\rm free}$ from Eq.(75) where the pressure of the jet equals the pressure of the external medium. Following the above arguments the jet speed after the shock is then approximately 1/7 of the sound speed i.e.

$$\beta^*_{\rm lobe} \gtrsim 1/\sqrt{3}/7 = 0.08, \tag{78}$$

close to estimated speeds in hotspots (Mesenheimer 1992). We obtain an optically thin spectrum for the whole observable frequency range

$$L^*_{\rm lobe} \;=\; 1.8\cdot 10^{34}\,\frac{\rm erg}{\rm s\,Hz}\,\left(\frac{\rm GHz}{\nu}\right)^{0.5} \tag{79}$$

[3] This is only valid as long the jets all see the same external pressure. A low power jet may terminate much earlier in a region, where the external pressure is slightly different.

$$\cdot \frac{\beta_{\mathrm{j}}^{\frac{1}{4}} P_{-12}^{\frac{1}{4}} x'_{\mathrm{e},100} \left(q_{\mathrm{j}/\mathrm{l}} L_{46}\right)^{\frac{3}{2}}}{\gamma_{\mathrm{j},5}^{\frac{7}{4}} u_3^{\frac{3}{4}}}$$

where the amplification is only due to the compression of the plasma. As expected, the extended (lobe) emission dominates the total flux at and below GHz frequencies. At these low magnetic fields we need very high Lorentz factors of the order 10^4 to 10^6 to explain the observed spectrum in the GHz range and beyond. A low-frequency turn-over could be visible at low MHz frequencies. It is noteworthy that core and lobe emission show a comparable scaling with accretion rate and $\gamma_{\mathrm{min,e}}$. The core to lobe luminosity ratio

$$\frac{L_{\nu_s}}{L_{\mathrm{lobe}}} = 0.07\, P_{-12}^{-\frac{1}{4}} \cdot \left(\frac{u_3 \sin i}{\beta_{\mathrm{j}} x'_{\mathrm{e},100} \sqrt{\gamma_{\mathrm{j},5} q_{\mathrm{j}/\mathrm{l}} L_{46}}}\right)^{\frac{1}{6}} \left(\frac{\nu}{\mathrm{GHz}}\right)^{0.5}. \quad (80)$$

is fairly insensitive to parameter changes. The latter as an observed quantity is of course a strong function of the Doppler factor and the luminosities and frequencies compared in Eq.(80) are frequencies in the rest frame of the flow. As cores probably are boosted and hotspots not, comparing lobe flux and core flux at the same *observed* frequency may therefore be misleading. In quasars where as a consequence of the unification scheme the Doppler factors are assumed to be of order unity, the core/lobe ratios indeed scatter around the value given above (see Paper II) whereas in FRII radio galaxies it is more then a factor 10 lower.

Allthough the values for the lobes we get are sufficiently close to the real world – especially with regard to the giant jump over several orders of magnitudes from cores to lobes – one should be very cautious in their interpretation: our equations describe the lobes as homogenous bubbles radiating uniformly, but the observed morphology is very different. Usually the brightness profiles peak towards a central hotspot. One therefore should understand our values only as crude averages and magnetic field and pressure in the central regions will definitively be higher.

Finally we want to calculate the expected luminosity of a non-maximal jet if it terminates at the same distance as a maximal one (Eq. 76). Using the same assumptions as before we get

$$L_{\mathrm{lobe}} = 2\cdot 10^{28}\,\frac{\mathrm{erg}}{\mathrm{s\,Hz}} \left(\frac{\mathrm{GHz}}{\nu}\right)^{0.5} \cdot \frac{\beta_{\mathrm{j}}^{\frac{1}{4}} P_{-12}^{\frac{1}{4}} f^{\frac{11}{8}} x_{\mathrm{e}}'^{\frac{19}{8}} \left(q_{\mathrm{j}/\mathrm{l}} L_{46}\right)^{\frac{3}{2}}}{\gamma_{\mathrm{j},5}^{\frac{7}{4}} u_3^{\frac{5}{8}}}. \quad (81)$$

This is a factor 1000 fainter than the already faint cores of such a jet. Therefore it seems almost impossible to ever detect radio emission from a putative lobe of non-maximal jets.

4. Inverse Compton scattering

4.1. Compton losses

Relativistic electrons in a jet produce not only synchrotron emission but will also upscatter photons via inverse Compton scattering. This leads to energy losses in the electron population and to the appearance of high energy emission in X-ray bands and beyond. Especially the scattering of their synchrotron photons (synchrotron self Compton effect – SSC) is an inevitable effect. A general result is that energy losses due to sychrotron radiation $\dot{E}_{\mathrm{sync}}$ and due to Compton scattering $\dot{E}_{\mathrm{comp}}$ are proportional where the proportionality factor is given by the ratios of the energy densities of magnetic field U_{B} and photons $\dot{E}_{\mathrm{ph}}$ in the rest frame of the jet

$$\frac{\dot{E}_{\mathrm{sync}}}{\dot{E}_{\mathrm{comp}}} = \frac{U_{\mathrm{B}}}{U_{\mathrm{ph}}}. \quad (82)$$

For the SSC effect this translates into the condition that locally the energy density of synchrotron photons dE_{sync}/dV has to be substantially lower than the magnetic field energy density to inhibit strong Compton losses. This condition is automatically fulfilled at distances larger than $Z^*_{\mathrm{min},1}$ (Eq. 66) – the distance where a large fraction of the internal energy is dissipated by synchrotron emission. At smaller scales the energy density in synchrotron photons would locally exceed the magnetic field energy density. SSC losses would increase this energy loss even further making acceleration of relativistic particles to the desired high energies at smaller scales impossible. On the other hand Compton scattering will give an additional factor < 2 at $Z^*_{\mathrm{min},1}$ so that at larger scales ($\gtrsim 10^{17}$ cm) SSC losses, like sychrotron losses, are no longer important for the energy budget of the electron population.

Another source for photons is of course the disk with a photon energy density $U_{\mathrm{ph,disk}} = 10^{46}\,\mathrm{erg/sec}\; L_{46}/(4\pi z^2 R_{\mathrm{g}}^2 c)$. Comparing this with $U_{\mathrm{B,jet}} = \gamma_{\mathrm{j}} B^2/8\pi$ and Eqs.(19&46) in the laboratoy frame we find that

$$\left(\frac{U_{\mathrm{B,jet}}}{U_{\mathrm{ph,disk}}}\right)^* = 7.5\, q_{\mathrm{j}/\mathrm{l}}\, \frac{\gamma_{\mathrm{j},5}\beta_{\mathrm{j}}}{u_3} \quad (83)$$

is a constant ratio and of the same order as $q_{\mathrm{j}/\mathrm{l}}$. For a non-maximal jet the ratio is a factor 2 higher. This result is intuitively clear as it reflects the basic assumptions of the model. The implications of a high energy density in disk photons are already know for a long time (Abramowicz & Piran 1980, Phinney 1982) because it provides a strong limit for the Lorentz factors in the jet close to the disk. From our simple equation we can conclude that, as long as $q_{\mathrm{j}/\mathrm{l}}$ is in the range $0.1 - 1$, synchrotron losses and Compton losses due to disk photons are comparable and Eqs. (64&65) state that the maximum Lorentz factor permitted by synchrotron losses in the very vicinity of the disk is of the order 10. As Compton scattering of disk radiation will energetically be at least equally important, these limits will become even more stringent if one would consider both. The limit $\gamma \lesssim 10$ is of the order of the bulk Lorentz factor of the jet – which usually is negligible compared to the electron Lorentz factors – so that close to the disk roughly the same process will constrain the bulk jet velocity as well (see also Melia & Königl 1989) because internal energy flow and kinetic energy flow are comparable. And indeed one finds that jet Lorentz factors usually derived are not $\gg 10$.

The scattering of the disk photons will result in a considerable gamma-ray spectrum but which can be seen only if the inclination angle is low. This point was discussed in detail by Dermer & Schlickeiser (1993). Here, we only note that the anisotropy of the disk radiation and the presence of an additional isotropic radiation field (Broad Line Region) complicate the analysis considerably. The energy loss equation (3.21) of Dermer & Schlickeiser however is basically the same as our Equation (83) if one considers the magnetic field gradient.

In our argumentation we have translated these loss mechanisms always into limits for jet parameters. Of course, if there is a persistent acceleration mechanism (for relativistic particles or bulk motion) at work it could be possible to dissipate a large fraction of the jet energy already at sub-parsce scales leading to strong high energy emission. On the other hand this would also lead to a reduction of the radio emission below what is seen in radio loud quasars because most of the energy would be lost before the jet starts to radiate in radio wavelengths. Radio weak quasars on the other hand do not show any signs of strongly enhanced gamma-ray emission.

4.2. SSC emission

Compton scattering is not only important as an energy loss mechanism but the synchrotron self Compton effect also is of great interest for the interpretation of quasar X-ray spectra (Jones et al. 1974, Königl 1981, Ghisellini et al. 1985, Marscher 1983 & 1987) where it generally is believed to be the relevant emission mechanism. In this paper we do not intend to present a thorough study of SSC emission as this was done in depth in the papers mentioned above. Most of these models, however, invoke a large number of parameters to fit observed spectra. Our model presented here will be contained in one of the previous SSC models as we have not changed the basic ingredients of jet models relevant for calculating the SSC spectrum; it is only that we are much more constrained in our choice of parameters by incorporating the accretion disk into a consistent physical picture of the quasar (jet-)emission. Hence, we do not expect results unheard of before. Nevertheless we briefly want to discuss the expected SSC emission from our model to get a feeling where to place it within the known jet models.

For given electron and photon distributions (Eqs. 7&47), the emissivity of inverse Compton scattering of a synchrotron powerlaw spectrum with $p = 2$ is roughly given by (Blumenthal & Gould 1970; Rybicky & Lightman 1979, Eq. 7.29a)

$$\epsilon_{\rm ssc} = 0.53\,\sigma_{\rm Th} c K_{\rm j} \epsilon_{\rm sync}(\nu_{\rm x}) r_{\rm j}\,(R_{\rm g}/c) \ln\left(\nu_{\rm r,1}/\nu_{\rm r,2}\right). \qquad (84)$$

The limits of the powerlaw are given by $\nu_{\rm x,1} = 4\gamma_{\rm e,min}^2 h\nu_{\rm r,1}$ and $\nu_{\rm x,2} = 4\gamma_{\rm e,max}^2 h\nu_{\rm r,2}$ where we have assumed that the synchrotron spectrum is given by a powerlaw between the two radio frequencies $\nu_{\rm r,1}$ and $\nu_{\rm r,2}$. For simplicity we set $\gamma_{\rm e,max} = 100\gamma_{\rm e,min}$. The frequency of the scattered X-ray spectrum is $\nu_{\rm x}$. We ignore the corrections introduced by the Klein-Nishina cross section and note that for a powerlaw distribution of the seed photons Eq.(47) overestimates the flux by a factor ~ 3 near the cut-offs.

Because we deal with a scattering process, where the total emission is given by the product of photon energy density and electron energy density, Eq. (84) will have a steeper gradient along the jet than the synchrotron emissivity and because of the relatively flat local SSC spectrum the total X-ray spectrum of the jet will be dominated by a single region in the jet. This is in marked contrast to the radio spectrum which is produced by different regions. If we integrate Eq. (84) analogous to the synchrotron emission (Eq. 54) along the jet, we obtain

$$L^*_{\nu_{\rm x},{\rm SSC}}(z_{\rm x}) = 2.0\cdot 10^{28}\,\frac{\rm erg}{\rm s\,Hz}\,\frac{{x'_{\rm e,100}}^2 (q_{\rm j/l}L_{46})^{\frac{11}{4}}}{\beta_{\rm j}\gamma_{\rm j,5}^3 u_3^{\frac{3}{4}}} \cdot\left(\frac{R_{\rm g} z_{\rm x}}{10^{17}{\rm cm}}\right)^{-\frac{3}{2}}\left(\frac{h\nu_{\rm x}}{\rm keV}\right)^{-\frac{1}{2}} \qquad (85)$$

where $z_{\rm x} R_{\rm g}$ is the distance in the jet where the SSC emission starts. For the integration we have considered only the locally produced $\nu^{-\frac{1}{2}}$ synchrotron emission as target photons for the relativistic electrons. Consideration of non-local cone emission will introduce an additional highly anisotropic, highly energetic, but much weaker photon flux component. As limits of the photon spectrum $\nu_{\rm r,1|2}$ we took the characteristic frequencies (Eq. 63&69) of the electrons with Lorentz factors $\gamma_{\rm e,min}$ and $\gamma_{\rm e,max}$ respectively. For this calculation the synchrotron-self absorption frequency is not appropriate because the absorption length scale $1/\kappa_{\rm sync}$ is much larger than the gyroradii of the scattering electrons; but we have shown before (Eq. 70) that self-absorption and characteristic frequency become equal if $\gamma_{\rm e,min} \sim 100$. The electrons in the jet might also see the low frequency $\nu^{\frac{1}{3}}$ spectrum below $\nu_{\rm r,1}$ which may extend the SSC spectrum to lower energies. Actually the situation is very complicated (see Sec. 4.3) as the plasma is optically thick to syncrotron at some frequencies but can cool by Compton scattering. It is not clear how the real local spectrum and the real, stationary electron distribution will look like.

To predict the SSC spectrum from a jet model one probably would have to discuss the evolution of the electron distribution along the jet to find the exact position z_x of the SSC emission region. Fortunately, we have argued above that the energetic component of the electron distribution which starts at $\gamma_{\rm e,min} \simeq 100$ can not be produced very close to the disk as it would suffer strong losses from synchrotron radiation and Compton scattering of disk photons. We thus can take the distances $Z^*_{\rm min,1}$ or $Z^*_{\rm min,2}$ (Eqs. 66&67), where synchrotron losses become negligible and the 'loud' electron distribution can be produced, as a lower limit for $z_x R_g$. $Z^*_{\rm min,1}$ inserted in the SSC jet emission formula (Eq. 85) yields

$$L^*_{\nu_{\rm x},\rm SSC} \lesssim 6.2\cdot 10^{28}\,\frac{\rm erg}{\rm s\,Hz}\,\eta_{03}x_{\rm e}'^{\frac{1}{4}}u_3^{\frac{5}{8}}\gamma_{\rm j,5}^{\frac{1}{4}}\beta_{\rm j}^{-\frac{1}{8}} \cdot(q_{\rm j/l}L_{46})^{\frac{9}{8}}\left(\frac{h\nu_{\rm x}}{\rm keV}\right)^{-\frac{1}{2}}. \tag{86}$$

To get the observed fluxes one has to do the same transformation from the jet frame into the observers frame (Eqs. 55) as for the radio emission.

This equation has the nice property that the X-ray luminosity scales with the radio core luminosity as $L^*_{\nu_{\rm x},SSC} \propto L^{*\;0.79}_{\nu_{\rm s}}$ which is in agreement with the observational finding that $L^*_{\nu_{\rm x},X-ray} \propto L^{*\;\;0.71\pm0.7}_{\nu_{\rm s},\rm radio}$ (Kembhavi et al 1986). However, the ratio between X-ray and radio flux

$$\frac{L^*_{\nu_{\rm x},SSC}}{L^*_{\nu_{\rm s}}} = 5\cdot 10^{-5}\,\frac{\beta_{\rm j}^{\frac{7}{24}}\gamma_{\rm j,5}^{\frac{25}{12}}u_3^{\frac{29}{24}}}{x'^{\;\frac{7}{12}}_{\rm e,100}(q_{\rm j/l}L_{46})^{\frac{7}{24}}}\left(\frac{h\nu_{\rm x}}{\rm keV}\right)^{-\frac{1}{2}}. \tag{87}$$

is a bit too high. If we go a bit further out along the jet to the distance $Z^*_{\rm min,2}$, where the electron loss time is reduced sufficiently, we find

$$L^*_{\nu_{\rm x},\rm SSC} \lesssim 7.9\cdot 10^{26}\,\frac{\rm erg}{\rm s\,Hz}\,\gamma_{\rm e,min}^{\frac{1}{2}}x_{\rm e}^2u_3^{\frac{3}{4}}\gamma_{\rm j,5}^{-\frac{3}{2}}\beta_{\rm j}^{-\frac{1}{8}} \cdot(q_{\rm j/l}L_{46})^{\frac{5}{4}}\left(\frac{h\nu_{\rm x}}{\rm keV}\right)^{-\frac{1}{2}}. \tag{88}$$

The ratio

$$\frac{L^*_{\nu_{\rm x},SSC}}{L^*_{\nu_{\rm s}}} \lesssim 6\cdot 10^{-7}\,\frac{\beta_{\rm j}^{\frac{1}{6}}\gamma_{\rm j,5}^{\frac{1}{3}}u_3^{\frac{4}{3}}x_{\rm e}^{\frac{7}{6}}}{\gamma_{\rm e,100}^{\frac{1}{3}}(q_{\rm j/l}L_{46})^{\frac{1}{6}}}\left(\frac{h\nu_{\rm x}}{\rm keV}\right)^{-\frac{1}{2}}. \tag{89}$$

is now compatible with the observed ratio of a few 10^{-7} (see Brunner et al. 1994) especially if one takes the transformations into the observers frame and a more precise SSC emissivity into account.

The peak of the SSC spectrum (i.e. the lower limit of the powerlaw) corresponding to the distance $Z^*_{\rm min,2}$ is

$$\nu_{\rm x,1} \approx 0.01\,({\rm keV}/h)\;\gamma^3_{\rm e,100}\beta_{\rm j}\gamma_{\rm j,5}u_3^{\frac{1}{2}}\sqrt{q_{\rm j/l}L_{46}}, \tag{90}$$

which means that if $\gamma_{\rm min,e}$ is only a bit higher than 100, the spectrum observed in ROSAT bands may be below the turnover of the SSC spectrum (implied by the low energy cut-off in the energy distribution). As the turnover can be very soft this could explain the very flat, sometimes inverted, (flux) spectra seen in quasars. The spectrum may well extend beyond energies of a few MeV.

4.3. SSC emission from the nozzle

To conclude the discussion of SSC emission we want to mention one interesting aspect of our concept. We can exclude from energy loss arguments that the highly energetic electron distribution with $\gamma_{\rm e,min} \gtrsim 100$, that makes a jet radio loud, is produced at the base of the jet. However, it might well be that there is a primary electron distribution of the plasma electrons which starts at low energies ($\gamma_{\rm e,min} \gtrsim 1$, $x_{\rm e} \lesssim 1$) and was already accelerated in the nozzle. Synchrotron emission of these electrons would be completely self-absorbed in the inner regions and be dominated by a secondary electron population ($\gamma_{\rm min,e} \gtrsim 100$) further out. The situation in the nozzle could either lead to a "synchrotron boiler" (Ghiselini et al. 1988) where electrons are cooked up to a thermal energy distribution – providing another mechanism to produce a kind of low energy cut-off – or the electrons would cool by SSC emission and produce a visible signature. If we now apply our SSC formula to a cylindrical region of radius $r_{\rm nozz}$ and height $z_{\rm nozz}$ with our parameters for the nozzle and $\gamma_{\rm e,min} \approx 1$ we find

$$L^*_{\nu_{\rm x},nozz} = 7.7\cdot 10^{27}\,\frac{\rm erg}{\rm s\,Hz}\,\frac{x_{\rm e}'(q_{\rm j/l}L_{46})^2}{\beta_{\rm j}^{\frac{11}{4}}\gamma_{\rm j,5}^{\frac{11}{2}}u_3^{\frac{3}{4}}m_8^{\frac{3}{2}}} \cdot\left(\frac{z_{\rm nozz}}{r_{\rm nozz}^{\frac{5}{2}}}\right)\left(\frac{h\nu_{\rm x}}{\rm keV}\right)^{-\frac{1}{2}}. \tag{91}$$

Although this depends strongly on the geometry of the nozzle and the Lorentz factor of the jet one should check if such a component could be present as well. Depending on the maximal Lorentz factor of these electrons ($\lesssim 10-100$) the spectrum could extend up to a few keV and would probably be steeper than $\nu^{-\frac{1}{2}}$ because of energy losses. If our notion of initially identical jets in radio loud and radio weak quasars, which later develop different electron populations, is correct such a signature would be common to radio loud and radio weak jets. The former would show an additional spectral component from the region at $Z^*_{\rm min,2}$, which could well dominate the nozzle emission, while the latter are likely to show only the steeper nozzle emission. Seen under small inclination angles radio weak quasars with SSC emission from the nozzle would exhibit strongly boosted X-ray emission and a still boosted but nevertheless much weaker radio emission. An application of this idea to the explanation of the large number of X-ray selected BL Lacs if compared to radio selected BL Lacs (Maraschi et al. 1992) seems possible but remains speculative at this point.

5. Disk and nozzle

After analyzing the jet and its energy demand we now want to discuss possible mechanisms for the jet production in relation to standard accretion disk theory (Novikov & Thorne 1973, Shakura & Sunyaev 1973). As said in the beginning, we have no idea, how the jet nozzle works and what process is responsible for the acceleration of the plasma. Still, we can give a crude description of the most likely scenario and test its feasibility.

The jet should start somewhere in the inner region of the disk between the innermost radius of the disk $r_{\rm in}$ and a point $r_{\rm nozz}$ furter out – the footpoint of the jet. What is a characteristic value for the dimensions of this part of the jet? Following standard accretion disk theory (Novikov & Thorne 1973) the inner radius of the disk will be given by the last marginal stable radius $r_{\rm ms}$ around the black hole. Following our symbiosis assumption a natural choice for the footpoint of the jet would be a radius close to the region where the inner boundary layer becomes important. Only in this region a disk really might require the presence of a jet. One guess would be to take the radius $r_{\rm max}$, where in standard accretion disk theory the radial run of the dissipation rate has its maximum. This point depends only on the Kerr parameter a (angular momentum) of the BH as shown in Fig. 1. The region between $r_{\rm max}$ and $r_{\rm in}$ is only poorly described by standard accretion disk theory and is partially unphysical (e.g. gas pressure and temperature decline rapidly to zero). Here magnetic processes and boundary effects of the black hole will dominate the disk – if a jet is produced this is the most likely place where it might happen. Moreover $r_{\rm max}$ is also the characteristic scale of all disk properties, as close to this value all radial functions of the disk peak.

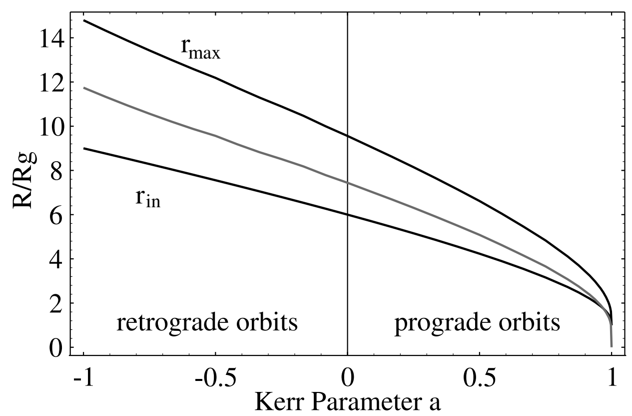

Fig. 1. The full lines give the inner disk radius and the radius $r_{\rm max}$ of the disk where the energy dissipation has its maximum as a function of the angular momentum $a \cdot R_{\rm g} M_{\bullet} c$ of the black hole. The grey line is an effective radius defined as $\sqrt{r_{\rm max}^2 - r_{\rm ms}^2}$ used to describe a filled cylinder with volume equivalent to a hollow cylinder with inner radius $r_{\rm max}$.

To get a feeling for the possible feeding mechanism of the jet, we calculate the maximal radial magnetic energy flux permitted in a thin accretion disk. To have a disk, the magnetic pressure should always be smaller than the total gas pressure. An upper limit for the maximum energy density of the magnetic field is given by the maximum total gas pressure at $r_{\rm max}$. In the inner part of radiation pressure supported disks this is of the order $10^3 - 10^4$ Gauss and depends only on the mass of the central black hole and its angular momentum parameter a hidden in the relativistic correction factors $\mathcal{A}, \mathcal{B}$ and $\mathcal{E}$. The derivation of the equations for standard relativistic accretion disks and the definition of the correction factors can be found in Novikov & Thorne (1973).

$$B_{\rm disk,max} = 1.2 \cdot 10^4\,{\rm Gauss}\,\frac{\sqrt{m_8}}{r^{\frac{3}{4}}}\frac{\mathcal{B}\sqrt{\mathcal{C}}}{\mathcal{A}} \tag{92}$$

This value of the magnetic field is close to the value required at the base of the maximal jet flow and for disks accreting close to the Eddington luminosity the scaling of magnetic fields in jet and disk would be the same. What is, however, more interesting is to compare the maximally possible radial magnetic energy flow through the accretion disk

$$\begin{aligned} Q_{\rm B,disk} &= B_{\rm max}^2/(8\pi) \cdot V_{\rm r}\, 2\pi r_{\rm max}\, z_{\rm disk}\, R_{\rm g}^2 \\ &= 1.9 \cdot 10^{46} \alpha \frac{\dot{m}_{\rm disk}^2}{m_8^3 r_{\rm max}^3} \frac{\mathcal{A}^2 \mathcal{Q}^2}{\mathcal{B}^4 \mathcal{D}^{\frac{3}{2}} \mathcal{E}} \frac{\rm erg}{\rm sec}, \end{aligned} \tag{93}$$

where $z_{\rm disk}$ is the disk height, $V_{\rm r}$ the radial velocity of the acretion flow and α is the Shakura & Sunyaev (1973) disk parameter, with the magnetic energy flow in the maximal jet

$$Q_{\rm B,jet} = 1/6 \cdot 10^{46}\,{\rm erg/sec}\; q_{\rm j/l} L_{46}/u_3 \tag{94}$$

yielding

$$\frac{Q_{\rm B,disk}}{Q_{\rm B,jet}} = \xi(a) \frac{\alpha u_3}{q_{\rm j} r_{\rm max}^3} \left(\frac{\dot{m}_{\rm disk}}{m_8}\right)^2. \tag{95}$$

The function $\xi(a)$ is evaluated and plotted in Fig. 2. We see that for radio loud jets the energy requirements are extremely high and exceed the maximum magnetic field flow allowed in the disk in all cases. Even though $q_{\rm j}$ may be as small as 0.1 and below, the limit is still very strong, as the viscosity parameter usually is assumed to be $\alpha \lesssim 0.1$ and additionally the accretion rate is already slightly above the Eddington limit. The Galactic Center source Sgr A* would lie more than 10 orders of magnitude below any allowed state. Thus radial accretion plus local amplification of the magnetic field seems very unlikely because it can not provide enough energy for the jet.

In this case we only have the choice to postulate that the magnetic field transported by the jet is produced locally at the footpoint of the jet in the disk by the dissipa-

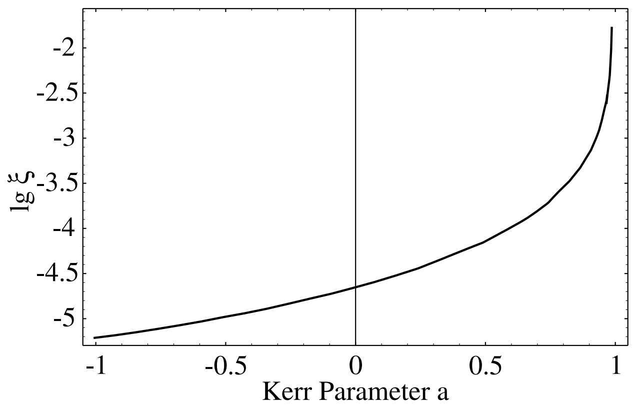

Fig. 2. The ratio ξ of the maximal radial magnetic energy flow in the disk compared to the magnetic energy flow in the jet for different Kerr parameters a and the parameters shown in Eq.(95).

tion processes. *In its inner region the disk* dissipates[4] *into a jet and not into heat.* With our parametrization we have already ensured that this is energetically possible – even in Sgr A*. This is not a completely surprising result, because one finding of accretion disk theory is that the dominant energy transport is in the vertical (local dissipation of gravitational energy) and not in the radial direction. If the jet-energy is a high fraction of the total accretion power than only a process linked to the dissipation process itself can provide us with enough energy over a long time-scale.

Common speculations for the dissipation process in accretion disks often invoke magnetic fields. A combination of dynamo processes (creating magnetic field) and reconnection (destroying magnetic field) could be a possible mechanism. If close to the boundary layer the rate of the magnetic field produced exceeds the rate in which it can be destroyed then the only way to dissipate the energy and continue the accretion is to produce a jet.

To highlight the possible geometry of such a jet, we make a simple estimate. Suppose below a certain disk radius $r_{\rm nozz}$ all the energy to be dissipated is diverted into the formation of a jet (calling it $Q_{\rm jet}$) and above $r_{\rm nozz}$ all energy is dissipated into heat producing the disk luminosity ($L_{\rm disk}$). To how large radii does one have to go, in order to obtain a certain value $Q_{\rm jet}/L_{\rm disk}$? We can easily answer this question by integrating the dissipation rate

$$D_0 = \frac{3GM_\bullet \dot{M}_{\rm disk}}{8\pi R_{\rm disk}^3}\frac{\mathcal{Q}}{\mathcal{B}\sqrt{\mathcal{C}}} = 6.8\cdot 10^{45}\frac{\dot{m}_{\rm disk}}{r_{\rm disk}^3}\frac{\mathcal{Q}}{\mathcal{B}\sqrt{\mathcal{C}}}\frac{\rm erg}{{\rm s}\,R_{\rm g}^2} \quad (96)$$

separately over the inner and outer region and defining

$$Q_{\rm jet} = \int_{r_{\rm in}}^{r_{\rm nozz}} 4\pi r_{\rm disk} D_0 R_{\rm g}^2 {\rm d}r_{\rm disk} \quad (97)$$

[4] The term *dissipation* is probably no longer appropriate in such a context.

$$L_{\rm disk} = \int_{r_{\rm nozz}}^{\infty} 4\pi r_{\rm disk} D_0 R_{\rm g}^2 {\rm d}r_{\rm disk}. \quad (98)$$

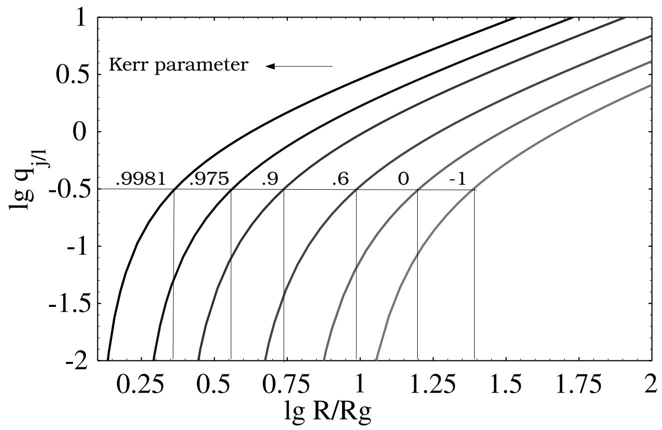

Fig. 3. Upper limit for the value $Q_{\rm jet}/L_{\rm disk}$ for given widths $r_{\rm nozz}$ of the jet at the disk, assuming that the dissipation energy of the disk inside the radius $r_{\rm nozz}$ is diverted completely into the jet ($Q_{\rm jet}$) and outside $r_{\rm nozz}$ is used to produce the disk luminosity ($L_{\rm disk}$). If in a more realistic case the separation between disk and jet is less stringent than for a fixed value of $Q_{\rm jet}/L_{\rm disk}$, the jet width has to be larger than the value indicated here. The different curves are for different Kerr parameters a (angular momenta) of the central black hole (-1 means retrograde orbits).

In Fig. 3 we show the ratio $Q_{\rm jet}/L_{\rm disk}$ as a function of $r_{\rm nozz}$. We find that even for high jet powers where $q_{\rm j/l}\simeq 1$, the jet can still be produced in the very inner regions of the disk. Once again this is no surprise as it is well known that most energy of an accretion disk is released very close to the center.

Of course in a realistic case the situation will be somewhat different and it is more likely that also in the inner parts of the disk only a fraction of the dissipated energy is used for the jet and not 100%. Therefore the radii indicated above should be taken as lower limits for the jet size or the values of $q_{\rm j/l}$ as upper limits.

Other pitfalls connected with this kind of argument are the unknown effects of the jet on the disk structure and the inner boundary conditions, which might change this picture quite a bit. There is also a possibility that the black hole itself can contribute to the jet production (Blandford & Znajek 1977) or the jet is produced in the very inner boundary layer. At the innermost orbits the particles still have a large amount of kinetic energy and it is unclear what fraction of this energy is swallowed by the black hole and what may escape. Despite this uncertainties it still seems justified to claim that for high ratios of $q_{\rm j/l}$ the jet probably is produced within a few gravitational radii from the black hole.

6. Discussion of the jet models

From our analysis in Sec. 2&3 we can interpret different combinations of parameters as conceptually different models for the radio emission of jets. They can be split in 5 different types as sketched in Fig. 4. We have a subdivision between maximal jets, where the internal sound speed reaches its maximal value $\beta_s \simeq 0.6c$ due to a large amount of magnetic energy and non-maximal jets with a sound speed substantially lower than $0.6c$. Moreover we may differentiate between radio loud and radio weak models according to their radiative efficiency or between high energy and low energy models according to their total energy. We label the individual models by a combination of letters representing their characteristic features (B=magnetic field, p=protons in equipartition, e=electrons in equipartition, Q=total energy flow).

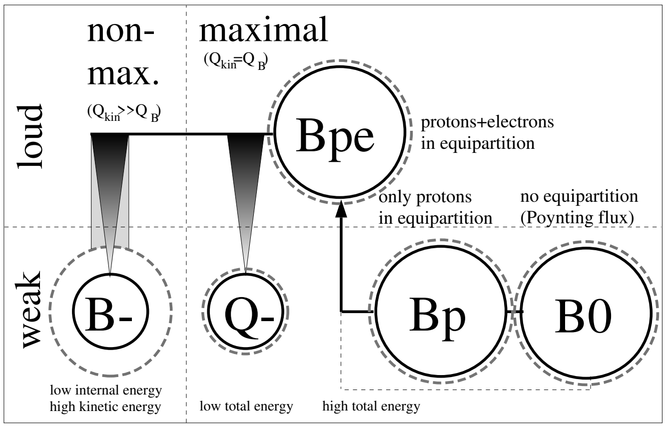

Fig. 4. The family of jet models as described in the text. The vertical axis indicates jet luminosity relative to the disk luminosity. Large circles mean high energy content, dashed circles are used for kinetic energy and full circles for internal energy.

Bpe: The high magnetic field is in equilibrium with electrons and protons ($k_{p+e} = 1$, $\mu_{p/e} \gtrsim 1$) requiring a minimum energy of the electrons of the order of 50 MeV ($\gamma_{min} \simeq 100/x_e$) or a large amount of $e^{\pm}$ pairs ($x_e \gtrsim 100$); maximal jet with high internal and kinetic energy flow ($q_{j/l} \lesssim 1$), radio loud.

Bp: The high magnetic field is in equilibrium with protons only and electrons carry much less energy ($\mu_{p/e} > 100$); maximal jet with high internal and kinetic energy flow ($q_{j/l} \lesssim 1$). This is the case if all thermal electrons are accelerated ($x_e \simeq 1$) but the powerlaw distribution starts at low energies ($\gamma_{min,e} \simeq 1$), radio weak.

B0: The high magnetic field is in equilibrium with neither the electrons nor the protons (Poynting flux, $k_{e+p} \lesssim 0.01$), maximal jet with high internal and kinetic energy flow ($q_{j/l} \lesssim 1$), radio weak or even quiet.

Q-: Like **Bpe** but with less total energy (therefore on an absolute scale a smaller magnetic field) relative to the disk luminosity ($q_{j/l} \ll 1$) and despite being radiatively very efficient classified as radio weak if compared to the disk.

B-: Non-maximal jet where the internal energy (magnetic field) is much lower than the kinetic energy ($\beta_s \sim 0.03c$) but electrons and protons are still in equipartition like in the **Bpe** model. This is the case if all thermal electrons are accelerated ($x_e \simeq 1$) but the powerlaw distribution starts at low energies ($\gamma_{min,e} \simeq 1$). The jet is radio weak and relatively narrow.

Only model **Bpe** is able to explain the powerful radio emission of the cores of radio loud quasars. This represents the most efficient case, where all parameters are set to their extremes (e.g. high jet power $q_{j/l} \simeq 1$ and high fraction of relativistic electrons $x_e \simeq 1$) and implies 'total equipartition', namely $L_{disk} \simeq Q_{jet} \gtrsim Q_B \simeq Q_e \simeq Q_p$ (the latter denotes the energy flow in relativisitic electrons and protons). Model **Bpe** is in principle also capable to explain distance and emission of extended lobes. One interesting consequence is that the relativistic electrons must have an unusual energy distribution peaking somewhere above 50 MeV inhibiting the usually assumed – but never observed – $\nu^{2.5}$ self-absorption spectrum at low frequencies. This quasi low-energy cut-off in the electron population was proposed first to avoid Faraday depolarization (Jones & O'Dell 1977, Wardle 1977) and later to explain the high kinetic powers of radio loud jets (Celotti & Fabian 1993). This minimum electron energy should be regarded as a lower limit as we only determine the product $x_e\gamma_{min,e}$. If only 10% of the electrons are relativistic then the minimum energy is a factor 10 higher. Perley et al. (1993) for example independently find a minimum Lorentz factor of $\gamma \sim 450$ for the electrons by fitting spectral aging models to high sensitivity data of Cygnus A.

The finding by Rawlings & Saunders (1991) that the extended lobes of radio jets carry a kinetic energy comparable to the disk luminosity together with the similar finding by us and Celotti & Fabian (1993) to explain the core and hotspot emision fix the problem at both sides (from cores to lobes) and set a well constrained framework for the understanding of radio jets.

For radio weak quasars the situation is more ambiguous. The results of Paper II and similar results by Miller et al. (1993) – the scaling of radio core emission with L_{disk} and the existence of possibly boosted radio weak objects – seem to support the idea that the radio emission in radio weak quasars is due to relativistic jets as well with velocities similar to radio loud jets. Principally all other models are equally well suitable to explain the compact radio emission of radio weak quasars (see Paper II). All except one (**Q-**) of these (radio-weak) models , however, still require a powerful jet with Q_{jet}/L_{disk} of the order unity mainly due to the power stored in bulk motion, relativistic protons and magnetic field.

In our simple picture also radio loud jets have to start as quiet jets (low electron energies, high magnetic fields) in order to avoid strong synchrotron losses and establish themselves as radio-loud through reacceleration a few 10^{16-17} cm away from the central black hole. One could suggest that all jets start with similar properties and follow a simple evolutionary track as depicted in Fig. 4. First one has a pure Poynting flux (**B0**) converging towards an equilibrium state where protons are (shock) accelerated (**Bp**) and finally relativistic electrons are produced (**Bpe**). Our motive to include the second stage is the minimum energy of the electrons of $\sim 50/x_{\rm e}$ MeV which is close to the energy of electron/positron pairs produced in the pion decay and one could further suggest that all electrons are in fact secondary pairs made by relativistic protons (Biermann & Strittmatter 1987, Mannheim & Biermann 1989, Sikora et al. 1987).

As this process should happen at least some 10^{16} cm from the origin it could be influenced by environmental effects, either because of the external photon flux or interactions of the jet with the ambient medium in a shear layer – a possible acceleration site (Ostrowski 1993). In radio quiet objects this mechanism simply might not be triggered towards an efficient production of secondaries and only the 'thermal' electrons are accelerated in the 'usual' way leaving the jet in the **Bp** or eben **B0** stage. Such a model avoids the need for a bimodal state of the disk to explain the difference between radio loud and radio weak jets (i.e. model **B**- and **Q**-). In fact Falcke, Gopal-Krishna & Biermann (1994) suggest that the reason for the different radio properties of AGN could simply be different kinds of power-dependent obscuring tori in different host galaxies which interact with the jet on the pc scale. This can explain the FR I/FR II transition as well as the radio loud/radio weak dichotomy without assuming different types of jets where the torus acts as the dense target for *pp* collisions. The idea that secondary pair production can be important in an astrophysical context was highlighted by Biermann, Strom & Falcke (1994) in an attempt to explain the low-frequency turn-over in the radio spectrum of the old nova GK Per.

An evolutionary scheme without secondaries (and without the second stage **Bp**) would be to assume that protons and plasma electrons both are accelerated by shock acceleration producing a flat electron spectrum ($p < 2$) until equipartition is reached at $\gamma \gtrsim 100$ where the distribution steepens again to $p = 2$. The only problem is that the injection of electrons is still unsolved. It is much more difficult to accelerate electrons and protons and if there is a certain threshold energy needed to shock accelerate electrons then the deficiency in the electron injection alone would be the prime reason for the dichotomy between radio loud and radio weak jets.

Finally we note that another natural explanation for high electron energies could be thermalization of electrons at high temperatures. If the bulk of the electron population is heated to temperatures $T_{\rm e} > 10^{11}$ K with an additional non-thermal power law tail we have exactly the distribution needed.

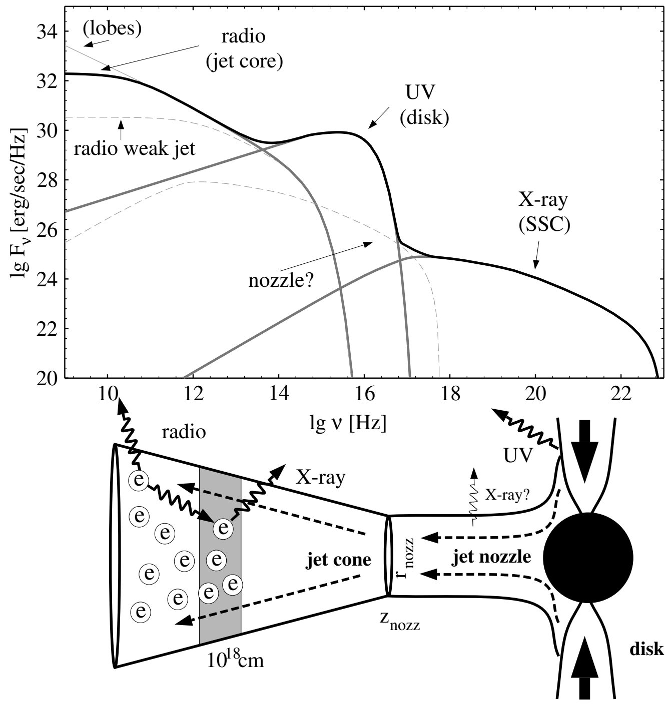

Fig. 5. Schematic broadband spectrum of a maximal jet-disk combination with three basic components (gray lines): core radio spectrum, disk spectrum, SSC spectrum. The full line gives the composite spectrum. Possible SSC emission from primary electrons in the nozzle is given by a dashed line as is the radio spectrum of a radio weak quasar. For comparison we also inserted a $\nu^{-.75}$ lobe spectrum (thin gray line). The core radio spectrum extends up to the frequency $\nu^*_{\rm max,2}$ corresponding to the spatial scale $Z^*_{\rm max,2}$ where it is assumed to steepen to ν^{-1}; a general cut-off at $10^{14.5}$ Hz is also assumed (Biermann & Strittmatter 1987). As parameters we took $m_8 = 1$, $L_{46} = 1$, $q_{\rm j/l} = 0.3$, $\gamma_{\rm min,e} = 300$, $\gamma_{\rm j} = 5$ $\ln(\gamma_{{\rm max},e}/\gamma_{{\rm min},e}) = 3.5$, $x_{\rm e} = 0.3$, for the nozzle (and the radio weak jet) we have assumed $\gamma_{\rm min,e} = 3$, $r_{\rm nozz} = 10$ and $z_{\rm nozz} = 100$. The inclination angle is $i = 35°$ so that the Doppler factor is unity. Boosted quasars will show a higher level of radio and X-ray emission in comparison to the blue bump. The disk spectrum for a maximally rotating Kerr hole ($a = 0.9981$) is taken from Falcke et al. (1993a).
Below the spectrum we sketched the general idea of the model where a part of the accretion disk flow is expelled by a jet. At a scale of 10^{17} cm a highly energetic electron population is produced being responsible for X-ray and radio emission in radio loud quasars. We suggest that the same picture holds for radio weak quasar but without the additional electron population.

The different models for radio weak jets could be distinguishable by their extended emission. One could speculate that models **B0** and **Bp** terminate at similar distances as their radio loud counterparts and produce dim extended emission like in FR I and FR II galaxies only a factor > 100 fainter. Here the only problem is whether in these jets – with a deficiency in electron acceleration – enough high energy electrons with $\gamma_e > 10^4$ are present to produce observable radio emission in the lobes. More promising therefore seem to be X-ray observations where one looks for interactions (shock fronts) with the IGM/ISM. Recent ROSAT observations of NGC 1275 (Böhringer et al. 1993) reveal such an X-ray emission and pressure equilibrium demands an proton/electron ratio of ~ 100 as in the **Bp** model.

The non-maximal jets (model **B-**) on the other hand would be virtually invisible as they either pierce through the ISM with a thin pencil-like beam or terminate further inside without noticeable radio emission leaving us only with the core emission. Finally, the low power jets (**Q-**) are likely to be be miniature editions of FR I galaxies on the kpc-scale.

7. Summary

In this paper we have applied the simple Blandford & Königl (1979) model for the flat spectrum core emission of radio jets in light of a link between the jet and an accretion disk as the source for energy and matter: we just demand mass and energy conservation of the jet-disk system as a whole. By expressing all quantities, including the plasma parameters, in terms of dimensionless parameters to be scaled with the disk accretion rate we describe the jet as an conically expanding relativistic plasma ($\Gamma = 4/3$) confined only by its own bulk velocity. This allows us to calculate a variety of observational features for different models. Despite many simplifications our jet model can describe the overall appearance of radio jets including sizes and fluxes of cores and lobes surprisingly well. Via the SSC effect this model naturlly accounts also for the X-ray emission of radio loud and possibly also for radio weak quasars. A schematic broadband spectrum is presented in Figure 5.

The models are limited by the requirement that the jet should not expel more matter and energy than is provided by the accretion disk. This limit strongly restricts models for radio-loud jets. At a disk (UV-bump) luminosity of 10^{46} erg/sec and core luminosities of $2 \cdot 10^{31} - 6 \cdot 10^{32}$ erg/sec/Hz for radio-loud quasars only the most efficient case is able to produce the observed radio emission. This implies a high total jet power ($Q_{\rm jet} \lesssim L_{\rm disk}$) where a large fraction of this total power is in magnetic fields and relativistic particles ('total equipartition'). Given the limited number of electrons from the accretion flow one needs an electron distribution starting at high energies ($\gtrsim 50$ MeV) and/or a large number of pairs. Heavy jet models with initial bulk velocities $\gamma_{\rm j} \gg 10$ seem to be excluded – the kinetic energy demand would be too high. We note that these conclusions are fairly independent of the details of any jet or disk model.

An electron distribution with low energy cut-off (> 50 MeV) is a natural consequence of hadronic interactions and the pion decay, so that the electrons might in fact be secondary pairs. The high amount of energy required to be channeled from the disk into the jet suggest that the jet is produced in the very inner parts of an accretion disk by a mechanism somehow linked to the dissipation process. The requirements on any acceleration process are very strong as its energizing efficiency must be very high compared to the total energy density of the jet. Although shock acceleration is in principle capable of such high efficiencies (e.g. Drury 1983) details of this process and especially its back reaction on the jet flow need to be investigated in more detailed.

The models described in this paper are also able to explain the compact radio emission in radio weak. In contrast to their radio-loud counterparts the parameters for radio-weak quasars can not be constrained much stronger and therefore the deeper reason for the dichotomy of quasars in radio-loud and radio-weak is still unclear. Yet, the possible answers can be reduced to two possibilities. Firstly, there might be a bimodality in the disk structure, especially at the boundary layer between disk and black hole (e.g. caused by different angular momenta of the black hole) leading to different power supplies for the jet (Models **Bpe** $\leftrightarrow$ **Q-** or **B-**) and secondly, the bimodality could be caused by different acceleration mechanisms for the electrons (Models **Bpe** $\leftrightarrow$ **Bp** or **B0**). The latter appears to be the most elegant way as it requires only changes in the microphysics which could easily be caused by environmental effects, e.g. by interactions between the jet and the ambient medium – or with the molecular torus – in a shear layer. This speculation then would suggest that jets in radio-loud quasars produce the dominant electron/positron population as secondary particles through hadronic interactions, whereas jets in radio-weak quasars contain only the directly accelerated population of electrons.

The model can be used without modification of the parameters to calculate the SSC emission from radio jets. The expected spectrum around one keV can be either flat ($\nu^{-0.5}$) or even inverted and is dominated by emission from one region at a distance of $\sim 10^{17}$ cm. SSC emission from the nozzle region could produce another spectral component wich might be of interest for X-ray emission of radio weak quasars and X-ray selected BL Lacs.

Acknowledgements. HF is supported by the DFG (Bi 191/9). We benefited from discussion with W. Duschl, T. Krichbaum and W. Krülls and comments of an anonymous referee.

References

Abramowicz, M.A., Piran, T. 1980, 241, L7
Biermann, P.L., Strittmatter, P.A. 1987, ApJ 322, 643
Biermann, P.L., Strom, R., Falcke, H. 1994, A&A in press
Blandford, R.D., Znajek, R.L. 1977, MNRAS 179, 433
Blumenthal, G.R., Gould, R.J. 1970, Rev. Mod. Phys. 42, 237
Böhringer, H., Voges, W., Fabian, A.C., Edge, A.C., Neumann, D.M. 1993, MNRAS 264, L25

Blandford, R.D., Königl, A. 1979, ApJ 232, 34
Bridle, A.H., Perley, R.A. 1984, ARAA 22, 319
Brunner, H., Lamer, G., Staubert, R., Worrall, D.M. 1994, A&A, in press
Camenzind 1986, A&A 156, 137
Celotti, A., Fabian, A. 1993, MNRAS 264, 228
Chini, R., Kreysa, E., Biermann, P.L. 1989a, A&A 219, 87
Chini, R., Biermann, P.L., Kreysa, E., Gemünd, H.-P. 1989b, A&A 221,L2
Dermer, C.D., Schlickeiser, R. 1993, ApJ 416, 458
Dermer, C.D., Schlickeiser, R. 1994, ApJS, in press
Drury, L.O'C. 1983, Rep. Prog. Phys. 46, 973
Falcke, H. 1994, PhD Thesis, RWF University Bonn
Falcke, H., Biermann, P. L. 1995, A&A submitted
Falcke, H., Biermann, P. L. 1993c, to appear in "Mass Transfer Induced Activity in Galaxies", Conference held in Lexington 1993, Shlosman, I. (ed.)
Falcke, H., Biermann, P. L., Duschl, W. J., Mezger, P. G. 1993a, A&A 270, 102
Falcke, H., Malkan, M., Biermann, P.L. 1994, A&A 298, 375
Falcke, H., Gopal-Krishna, Biermann, P.L. 1994, A&A 298, 395
Falcke, H., Mannheim, K., Biermann, P. L. 1993b, A&A 278, L1
Fanti, R., Fanti, C., Schilizzi, R.T. et al. 1990, A&A 231, 333
Ghisellini, G., Guilbert, P.W., Svensson, R. 1988, ApJ 334, L5
Ghisellini, G., Maraschi, L., Treves, A. 1985, ApJ 146, 204
Ghisellini, G., Padovani, P., Celotti, A., Maraschi, L. 1993, ApJ 407, 65
Haardt, F., Maraschi, L. 1991, ApJ 380, L51
Hartmann, D.L., Bertsch, D.L., Fichtel, C.E. et al. 1992, ApJ 385, L1
Jones, T.W., O'Dell, S.L. 1977, A&A 61, 29
Jones, T.W., O'Dell, S.L., Stein, W.A. 1974, ApJ 188, 353
Kellermann, K.I., Pauliny-Toth, I.I.K. 1969, ApJ 155, L71
Kellermann, K.I., Sramek, R., Schmidt, M., Shaffer, D.B., Green, R. 1989, AJ 98, 1195
Kembhavi, A., Feigelson, E.D., Singh, K.P. 1986, MNRAS 220, 51
Königl, A. 1980, Phys. Fluids 23, 1083
Königl, A. 1981, ApJ 243, 700
Krichbaum T.P., Zensus J.A., Witzel A., Mezger P.G., Standke K. et al., 1993, A&A 274, L37
Lind, K.R., Blandford, R.D. 1985, ApJ 295, 358
Mannheim, K. 1993, A&A 269, 67
Mannheim, K., Biermann P.L. 1989, A&A 221, 211
Maraschi, L., Celotti, A., Ghisellini, G. 1992, in: "Physics of AGN", Springer Verlag, W. Duschl & S.J. Wagner (eds.), p. 605
Marscher, A.P., ApJ 264, 296
Marscher, A.P. 1987, in: "Superluminal Radio Sources", Cambridge University press, J.A. Zensus & T.J. Pearson (eds.), p. 280
Marscher, A.P. 1992, in: "Physics of AGN", Springer Verlag, W. Duschl & S.J. Wagner (eds.), p. 510
Marscher, A.P., Gear, W.K. 1985, ApJ 298, 114
Meisenheimer, K. 1992, in: "Physics of AGN", Springer Verlag, W. Duschl & S.J. Wagner (eds.), p. 525
Melia, F., Königl, A. 1989, ApJ 340, 162
Miller, P., Rawlings, S., Saunders, R. 1993, MNRAS 263, 425
Niemeyer, M., Biermann, P.L. 1993, A&A 297, 393
Novikov I.D., Thorne K.S., 1973, Black Hole Astrophysics. In: DeWitt C., DeWitt B. (eds.), Les astres occlus, Gordon & Breach, New York, p.343-450
Ostrowski, M. 1993, preprint
Perley, R.A., Carilli, C.L., Leahy, J.P. 1993, In: Jets in Extragalactic Radio Sources, eds. Röser & Meisenheimer, Springer Verlag, p.217
Phinney, E.S. 1982, MNRAS 198, 1109
Rawlings, S., Saunders, R. 1991, Nat 349, 138
Rybicki, G.B., Lightman, A.P. 1979, "Radiative Processes in Astrophysics", John Wiley & Sons, New York
Sikora, M., Kirk, J.G., Begelman, M.C., Schneider, P. 1987, ApJ 320, L81
Sun, W.H., Malkan, M. 1990, ApJ 346, 68
Thorne, K. S. 1974, ApJ 191, 507
Wardle, J.F.C. 1977, Nat 269, 563
Zdziarski, A.A., Ghisellini, G., George, I.M., Svensson, R., Fabian, A.C., Done, C. 1990, ApJ 363, L1

A. Appendix

Here we give some of the equations derived in the main body of the paper for a different electron powerlaw index of $p = 2.5$.

Eqs. (52,53)

$$z_{\rm ssa} = 10\,{\rm pc}\, \frac{{x'_{\rm e}}^{\frac{2}{13}} \beta_{\rm j}^{\frac{9}{26}} \left(q_{\rm j/l} L_{46}\right)^{\frac{17}{26}}}{\sqrt{u_3}\,\gamma_{\rm j,5}^{\frac{4}{13}} f^{\frac{2}{13}} \sin i^{\frac{4}{13}}} \frac{\rm GHz}{\nu_{\rm s,obs}/\mathcal{D}} \tag{A1}$$

$$z^*_{\rm ssa} = 35\,{\rm pc}\, \frac{{x'_{\rm e,100}}^{\frac{4}{13}} \beta_{\rm j}^{\frac{9}{26}} \left(q_{\rm j/l} L_{46}\right)^{\frac{17}{26}}}{\gamma_{\rm j,5}^{\frac{4}{13}} u_3^{\frac{9}{26}} \sin i^{\frac{4}{13}}} \frac{\rm GHz}{\nu_{\rm s,obs}/\mathcal{D}} \tag{A2}$$

Eqs. (56,57)

$$L_{\nu_{\rm s,obs}} = 5.8 \cdot 10^{30}\, \frac{\rm erg}{\rm s\,Hz} \left(q_{\rm j/l} L_{46}\right)^{\frac{18}{13}} \cdot \frac{\mathcal{D}^{\frac{29}{13}} \sin i_{\rm obs}^{\frac{3}{13}} f^{\frac{3}{26}} {x'_{\rm e}}^{\frac{23}{26}}}{\sqrt{u_3}\,\gamma_{\rm j,5}^{\frac{23}{13}} \beta_{\rm j}^{\frac{5}{13}}} \tag{A3}$$

$$L^*_{\nu_{\rm s,obs}} = 8.7 \cdot 10^{32}\, \frac{\rm erg}{\rm s\,Hz} \left(q_{\rm j/l} L_{46}\right)^{\frac{18}{13}} \cdot \frac{\mathcal{D}^{\frac{29}{13}} \sin i_{\rm obs}^{\frac{3}{13}} {x'_{\rm e,100}}^{\frac{10}{13}}}{\gamma_{\rm j,5}^{\frac{23}{13}} \beta_{\rm j}^{\frac{5}{13}} u_3^{\frac{8}{13}}} \tag{A4}$$

Eqs. (58,59)

$$T_{\rm b} = 3.7 \cdot 10^{10}\,{\rm K} \left(\frac{x'_{\rm e} q_{\rm j/l} L_{46}}{f \gamma_{\rm j,5}^2 \beta_{\rm j}}\right)^{\frac{1}{13}} \sin i^{\frac{11}{13}} \tag{A5}$$

$$T^*_{\rm b} = 6.6 \cdot 10^{10}\,{\rm K} \left(\frac{{x'_{\rm e,100}}^2 u_3 q_{\rm j/l} L_{46}}{\gamma_{\rm j,5}^2 \beta_{\rm j}}\right)^{\frac{1}{13}} \sin i^{\frac{11}{13}} \tag{A6}$$

Eqs. (61,62)

$$\nu_{\rm max} = 1.9 \cdot 10^{12}\,{\rm Hz}\ \eta_{03} \frac{f^{\frac{23}{26}} \gamma_{\rm j,5}^{\frac{23}{13}} \beta_{\rm j}^{\frac{5}{13}} {x'_{\rm e}}^{\frac{3}{26}} u_3^{\frac{3}{2}}}{\left(q_{\rm j/l} L_{46}\right)^{\frac{5}{13}} \sin i^{\frac{3}{13}}} \tag{A7}$$

$$\nu^*_{\rm max} \;=\; 1.9\cdot 10^{12}\,{\rm Hz}\;\eta_{03}\frac{\gamma_{\rm j,5}^{\frac{23}{13}}\beta_{\rm j}^{\frac{5}{13}}u_3^{\frac{8}{13}}}{{x'_{\rm e,100}}^{\frac{10}{13}}\left(q_{\rm j/l}L_{46}\right)^{\frac{5}{13}}\sin i^{\frac{3}{13}}} \quad ({\rm A8})$$

Eq. (70)

$$\frac{\nu^*_{\rm s}}{\nu^*_{\rm c}} = 1.6\;\gamma_{\rm min,100}^{-\frac{20}{13}}\left(\frac{q_{\rm j/l}L_{46}x_{\rm e}^2}{\beta_{\rm j}\gamma_{\rm j,5}^2\sin i^2}\right)^{\frac{2}{13}} \quad ({\rm A9})$$

Eq. (79)

$$L^*_{\rm lobe} \;=\; 3.3\cdot 10^{33}\,\frac{\rm erg}{\rm s\,Hz}\,\left(\frac{\rm GHz}{\nu}\right)^{0.75}\cdot \frac{\beta_{\rm j}^{\frac{3}{8}}P_{-12}^{\frac{3}{8}}x'_{\rm e,100}\left(q_{\rm j/l}L_{46}\right)^{\frac{3}{2}}}{\gamma_{\rm j,5}^{\frac{15}{8}}u_3^{\frac{7}{8}}} \quad ({\rm A10})$$

This article was processed by the author using Springer-Verlag LaTeX A&A style file *L-AA* version 3.